Journal of Mathematical Biology (2024) 88:33
https://doi.org/10.1007/s00285-024-02051-6

Mathematical Biology

The role of natural recovery category in malaria dynamics under saturated treatment

Jing Wang[1,2] · Hongyong Zhao[1,2] · Hao Wang[3]

Received: 19 July 2023 / Revised: 29 December 2023 / Accepted: 19 January 2024

Abstract

In the process of malaria transmission, natural recovery individuals are slightly infectious compared with infected individuals. Our concern is whether the infectivity of natural recovery category can be ignored in areas with limited medical resources, so as to reveal the epidemic pattern of malaria with simpler analysis. To achieve this, we incorporate saturated treatment into two-compartment and three-compartment models, and the infectivity of natural recovery category is only reflected in the latter. The non-spatial two-compartment model can admit backward bifurcation. Its spatial version does not possess rich dynamics. Besides, the non-spatial three-compartment model can undergo backward bifurcation, Hopf bifurcation and Bogdanov–Takens bifurcation. For spatial three-compartment model, due to the complexity of characteristic equation, we apply Shengjin's Distinguishing Means to realize stability analysis. Further, the model exhibits Turing instability, Hopf bifurcation and Turing–Hopf bifurcation. This makes the model may admit bistability or even tristability when its basic reproduction number less than one. Biologically, malaria may present a variety of epidemic trends, such as elimination or inhomogeneous distribution in space and periodic fluctuation in time of infectious populations. Notably, parameter regions are given to illustrate substitution effect of two-compartment model for three-compartment model in both

✉ Hongyong Zhao
hyzho1967@126.com

Jing Wang
wakwangjing@126.com

Hao Wang
hao8@ualberta.ca

1 School of Mathematics, Nanjing University of Aeronautics and Astronautics, Nanjing 211106, China

2 Key Laboratory of Mathematical Modelling and High Performance Computing of Air Vehicles (NUAA), MIIT, Nanjing 211106, China

3 Department of Mathematical and Statistical Sciences, University of Alberta, Edmonton, AB T6G 2G1, Canada

Published online: 27 February 2024

scenarios without or with spatial movement. Finally, spatial three-compartment model is used to present malaria transmission in Burundi. The application of efficiency index enables us to determine the most effective method to control the number of cases in different scenarios.

Keywords Malaria · Natural recovery category · Saturated treatment · Stability · Bifurcation · Substitution effect

Mathematics Subject Classification 34C23 · 35B35 · 35K57 · 37N25

1 Introduction

Malaria is a fatal disease spread to human population through contact with infected female *Anopheles* mosquitoes. Five kinds of *Plasmodium* are responsible for malaria, among which *Plasmodium falciparum* and *Plasmodium vivax* pose the greatest threat (Becker et al. 2010; World Health Organization 2023). Unfortunately, malaria is endemic in about 100 countries in the America, Southeast Asia and Africa (Gutierrez et al. 2015). About 247 million individuals were infected and 619 000 cases died in 2021 (World Health Organization 2023). Malaria directly threatens public health and has a huge adverse impact on local economies (Bai et al. 2018). It is therefore of great significance to study the transmission of malaria.

Mathematical modelling is a powerful tool to explain and predict epidemic trends. The mathematical model for malaria spread has a long history, first formed by Ross (1911) and then amended by Macdonald (1952, 1957). Thereafter, researchers have made significant progress in applying mathematical models to understand this disease (An and Jäger 2014; Lou and Zhao 2011; Takoutsing et al. 2014; Shi and Zhao 2021; Zhao et al. 2022; Shi et al. 2022, 2023; Wang et al. 2023a, b). In recent years, convenient transportation has facilitated the spatial diffusion of humans and vectors, which may contribute to the spread of malaria (Schlagenhauf 2004; Tatem et al. 2006). As far as we know, reaction-diffusion equations are often used to describe population movement (Xin and Wang 2021; Zha and Jiang 2023; Wang and Wang 2021; Xiang et al. 2023; Shen et al. 2023; Li et al. 2023; Zhang et al. 2023; Wang et al. 2022). Nevertheless, there are still several shortcomings in the current research on reaction-diffusion malaria model.

On the one hand, malaria is a curable infectious disease. In some areas of developing countries, with the expansion of scale for infected persons, it may not be possible to treat emerging cases in time as the shortage of medical resources (Gao et al. 2017; Laman et al. 2014; Mtove et al. 2018). Zhang et al. Zhang and Liu (2008) proposed a continuously differentiable function

$$T(I) = \frac{rI}{1+\alpha I},\ r > 0,\ \alpha \geq 0, \tag{1}$$

to represent the number of persons who recover from therapy. Here r denotes the cure rate, α stands for the extent of the delayed effect for treatment, and I is the number

of infected humans. Moreover, they defined the basic reproduction number R_0, and observed that with weak delayed effect for treatment, $R_0 = 1$ is a threshold condition of disease elimination; while the model underdoes backward bifurcation as such effect is strong. Later, the above treatment function was discussed in Gao et al. (2017); Zhou and Fan (2012); Zhou et al. (2014); Wang and Zhao (2022). However, little attention has been paid to the effect of saturated treatment on dynamics for reaction–diffusion model.

On the other hand, individuals who recover naturally contain low levels of gametes in the blood, which can infect mosquitoes (Bousema et al. 2010). In Wang and Zhao (2022), Lou and Zhao (2010), the authors incorporated this fact into model, and made dynamics analysis. But, they did not make further exploration. For example, what impact does ignoring the infectivity of natural recovery individuals have on dynamic behaviors? In addition, they also overlooked spatial movement. In view of these issues, we establish two-compartment and three-compartment reaction-diffusion models with saturated treatment, which correspond to ignoring and emphasizing the infectivity of natural recovery individuals, respectively. For completeness, their non-spatial versions are also introduced. Our aim is to investigate whether/when we can neglect the infectivity of these individuals in both scenarios without and with spatial diffusion. Concretely, in each scenario, explore (i) under what conditions two-component model can be used instead of three-component model; and (ii) under what conditions it is inevitable to investigate three-component model, since its dynamics are irreplaceable and differ significantly from that of two-component model.

The highlights and contributions of this work are briefly summarized as follows. For spatial three-compartment model, it is difficult to determine the signs of some coefficients related to the characteristic equation, which becomes an obstacle to stability analysis. Fortunately, the application of Shengjin's Distinguishing Means enables us to overcome this difficulty. Moreover, the normal form of Turing–Hopf bifurcation is given, in which the details are different from those of Turing–Hopf bifurcation for two-compartment one (Song et al. 2016). Spatial three-compartment model exhibits abundant dynamics near bifurcation point. That makes the model may allow tristability phenomena when its basic reproduction number less than one, which seems to be new discovery compared with the previous research on reaction-diffusion epidemic model (Sun 2012; Wang et al. 2018; Zhu and He 2022). What's more, in each scenario, two-compartment model may reveal, underestimate, overestimate or misjudge the prevalence of malaria compared to the three-compartment model. Note that in scenario without spatial diffusion, the misjudgment is caused by Hopf bifurcation and Bogdanov–Takens bifurcation in three-compartment model. However, in scenario with spatial diffusion, the misjudgment is caused by Turing instability, Hopf bifurcation and Turing–Hopf bifurcation in three-compartment model. These outcomes provide new insight into the impact of infectivity of natural recovery category on malaria transmission.

The rest of this paper is organized as follows. The two-compartment and three-compartment reaction-diffusion models are formulated in Sect. 2. In Sect. 3, two-compartment models without and with spatial diffusion are analyzed. Section 4 investigates three-compartment models without and with spatial diffusion. Further, parameter areas are given to illustrate substitution outcomes. In Sect. 5, the theoretical

results are verified by numerical simulations. Moreover, we compare two-compartment and three-compartment models in both scenarios without and with spatial movement. In Sect. 6, spatial three-compartment model is applied to present the transmission of malaria in Burundi. Finally, Sect. 7 presents a brief discussion.

2 Model formulation

We first formulate a three-compartment reaction-diffusion malaria model with saturation treatment. The human population is divided into three compartments: susceptible category $S_h(t,x)$, infected category $I_h(t,x)$ (the body contains schizozoites and gametophytes) and natural recovery category $R_h(t,x)$ (the body contains only gametophytes, while the individual is slightly contagious), where t and x represent time and position respectively. Assume that the total density for human population $N_H(t,x) = S_h(t,x) + I_h(t,x) + R_h(t,x)$ can be confirmed by

$$\frac{\partial N_H(t,x)}{\partial t} = d_1 \Delta N_H(t,x) + H - d_h N_H(t,x),\ t > 0,\ x \in \Omega, \tag{2}$$

where $d_1 > 0$ is the diffusion coefficient, H denotes the recruitment rate, d_h stands for the natural death rate for humans and Ω is the spatial habitat with smooth boundary $\partial\Omega$. For convenience, let $\Omega = (0, l\pi)$ with $l > 0$. For system (2), take homogeneous Neumann boundary condition

$$\frac{\partial N_H(t,x)}{\partial n} = 0,\ t > 0,\ x \in \partial\Omega, \tag{3}$$

in which n is the outward unit normal vector on $\partial\Omega$ and $\frac{\partial}{\partial n}$ represents the differentiation along n to $\partial\Omega$. System (2)–(3) allows a globally asymptotically stable steady state $N_h = \frac{H}{d_h}$ (Lou and Zhao 2011). In light of Bai et al. (2018); Shi and Zhao (2021); Xin and Wang (2021), suppose that the total density of human population stabilizes at N_h. The mosquito population consists of susceptible and infected classes with spatial densities $S_v(t,x)$ and $I_v(t,x)$, respectively. Let $N_V(t,x) = S_v(t,x) + I_v(t,x)$ be the total density for mosquitoes, which satisfies equation

$$\begin{cases} \dfrac{\partial N_V(t,x)}{\partial t} = d_2 \Delta N_V(t,x) + \Lambda - d_v N_V(t,x), & t > 0,\ x \in \Omega, \\ \dfrac{\partial N_V(t,x)}{\partial n} = 0, & t > 0,\ x \in \partial\Omega, \end{cases} \tag{4}$$

where $d_2 > 0$ is the diffusion coefficient, Λ denotes the recruitment rate and d_v represents the natural death rate for mosquitoes. Analogously, assume that the total density for mosquitoes stabilizes at $N_v = \frac{\Lambda}{d_v}$, which is consistent with Anita and Capasso (2012), Zha and Jiang (2023). Below, without causing confusion, remove (t,x) from the state variables. In addition, S_h and S_v are expressed as $N_h - I_h - R_h$ and $N_v - I_v$ respectively.

Susceptible humans acquire malaria via effective bite of infected mosquitoes at a rate $b\beta_h \frac{I_v}{N_h}$. It follows from Bousema et al. (2010) that treatment can significantly shorten the carrying time of gamete cells. The reasonable hypothesis is that if an infected person takes the medicine according to advice, then all parasites in the body will be cleared (An and Jäger 2014). Hence infected individuals enter into susceptible category at a rate $\frac{\delta}{1+\alpha I_h}$ and enter into natural recovery category at a rate r. Natural recovery persons become susceptible after gametophyte carrying period $\frac{1}{\upsilon}$. Besides, susceptible mosquitoes infect malaria at a rate $b\beta_v \frac{I_h+\theta R_h}{N_h}$ because of effective contact with infectious individuals. Flow diagram of malaria transmission is shown in Fig. 1a. See Table 1 for descriptions of all parameters. In view of the discussions above, introduce the following reaction-diffusion malaria model

$$\begin{cases} \dfrac{\partial I_h}{\partial t} = d_1 \Delta I_h + b\beta_h \dfrac{I_v}{N_h}(N_h - I_h - R_h) - \dfrac{\delta I_h}{1+\alpha I_h} - r I_h - d_h I_h, & t > 0,\ x \in \Omega, \\ \dfrac{\partial R_h}{\partial t} = d_1 \Delta R_h + r I_h - d_h R_h - \upsilon R_h, & t > 0,\ x \in \Omega, \\ \dfrac{\partial I_v}{\partial t} = d_2 \Delta I_v + b\beta_v \dfrac{I_h + \theta R_h}{N_h}(N_v - I_v) - d_v I_v, & t > 0,\ x \in \Omega, \\ \dfrac{\partial I_h}{\partial n} = \dfrac{\partial R_h}{\partial n} = \dfrac{\partial I_v}{\partial n} = 0, & t > 0,\ x \in \partial\Omega, \\ I_h(0,x) := I_h^0(x) \geq 0,\ R_h(0,x) := R_h^0(x) \geq 0, & \\ I_v(0,x) := I_v^0(x) \geq 0, & x \in \bar{\Omega}. \end{cases} \tag{5}$$

Since natural recovery class is slightly infectious in the process of malaria transmission (Wang and Zhao 2022; Lou and Zhao 2010), we are interested in whether neglecting the infectivity of natural recovery persons can simplify analysis and preserve dynamical behaviors of three-compartment model. In this case, natural recovery persons directly return to susceptible category. Figure 1b exhibits flow diagram of disease transmission. Accordingly, the following two-compartment model is obtained

$$\begin{cases} \dfrac{\partial I_h}{\partial t} = d_1 \Delta I_h + b\beta_h \dfrac{I_v}{N_h}(N_h - I_h) - \dfrac{\delta I_h}{1+\alpha I_h} - r I_h - d_h I_h, & t > 0,\ x \in \Omega, \\ \dfrac{\partial I_v}{\partial t} = d_2 \Delta I_v + b\beta_v \dfrac{I_h}{N_h}(N_v - I_v) - d_v I_v, & t > 0,\ x \in \Omega, \\ \dfrac{\partial I_h}{\partial n} = \dfrac{\partial I_v}{\partial n} = 0, & t > 0,\ x \in \partial\Omega, \\ I_h(0,x) := I_h^0(x) \geq 0,\ I_v(0,x) := I_v^0(x) \geq 0, & x \in \bar{\Omega}. \end{cases} \tag{6}$$

In the following, we devote ourselves to analyzing system (5), system (6) and corresponding non-spatial versions, so as to explore what impact will be caused by neglecting the infectivity of natural recovery individuals on malaria transmission?

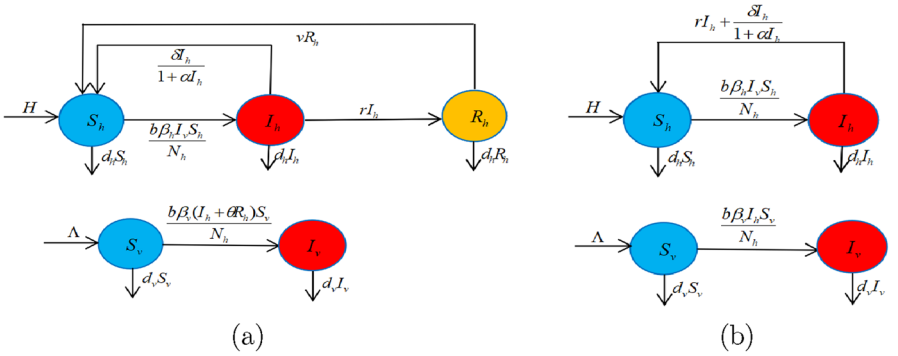

Fig. 1 Schematic diagram of malaria spread for **a** system (5) with $S_h = N_h - I_h - R_h$ and $S_v = N_v - I_v$ and **b** system (6) with $S_h = N_h - I_h$ and $S_v = N_v - I_v$

Table 1 Parameter descriptions

Parameter	Description
H	Recruitment rate of human population $((\text{km}^2\text{Day})^{-1})$
d_h	Natural death rate of human population (Day^{-1})
r	Natural recovery rate of human population (Day^{-1})
δ	Treatment recovery rate of human population (Day^{-1})
α	The extent of the delayed effect for treatment
$1/v$	Time for natural recovery individuals to carry gamete cells (Day)
θ	Infectious reduction factor
Λ	Recruitment rate of adult mosquitoes $((\text{km}^2\text{Day})^{-1})$
d_v	Natural death rate of adult mosquitoes (Day^{-1})
b	Biting rate of mosquitoes (Day^{-1})
β_v	Transmission probability from infected humans to susceptible mosquitoes
β_h	Transmission probability from infected mosquitoes to susceptible humans
d_1	Human diffusion rate $(\text{km}^2\text{Day}^{-1})$
d_2	Mosquito diffusion rate $(\text{km}^2\text{Day}^{-1})$

3 Dynamics analysis for system (6) and its non-spatial system

This part aims to explore the dynamical behaviors of system (6) and its non-spatial system. Firstly, the existence of equilibria is discussed, then the stability and bifurcation for non-spatial system are explored, and finally the stability for system (6) is analyzed.

With the aid of Lou and Zhao (2011), Shi and Zhao (2021), Shi et al. (2021), one acquires the following outcome.

Theorem 1 *System* (6) *possesses a unique global classical solution* $(I_h, I_v)^{\mathrm{T}}$ *for* $t \geq 0$, $x \in \bar{\Omega}$. *Moreover, if* $I_h^0(x) \not\equiv 0$, $I_v^0(x) \not\equiv 0$, *then* $I_h > 0$, $I_v > 0$ *for* $t > 0$, $x \in \bar{\Omega}$.

3.1 Existence of equilibria for system (6)

In this subsection, give the distribution of equilibria for system (6). Apparently, system (6) always has a disease-free equilibrium (DFE) $\bar{E}_0 = (0, 0)^{\mathrm{T}}$.

In light of Wang and Zhao (2012), introduce the basic reproduction number

$$\bar{\mathcal{R}}_M = \sqrt{\frac{b\beta_v N_v}{N_h} \cdot \frac{1}{r + d_h + \delta} \cdot b\beta_h \cdot \frac{1}{d_v}}. \tag{7}$$

Biologically, $\bar{\mathcal{R}}_M$ stands for the average number of secondary cases produced by one infected person or mosquito during its infection period in a completely susceptible population. The average number of infected mosquitoes generated by one infected person contacting mosquitoes at a rate $\frac{b\beta_v N_v}{N_h}$ during its infection period $\frac{1}{r+d_h+\delta}$ is $\frac{b\beta_v N_v}{N_h(r+d_h+\delta)}$. The average number of infected persons produced by an infected mosquito contacting humans at a rate $b\beta_h$ during its infection period $\frac{1}{d_v}$ is $\frac{b\beta_h}{d_v}$. As two generations are required to transmit malaria, $\bar{\mathcal{R}}_M$ is formula (7). Moreover, due to the fact that the delayed effect for treatment only occurs when there are a large number of infected individuals, the delayed effect for treatment does not affect $\bar{\mathcal{R}}_M$.

To simplify the discussion, denote $\bar{\mathcal{R}}_0 = (\bar{\mathcal{R}}_M)^2$. Apparently,

$$\bar{\mathcal{R}}_M > 1 \Leftrightarrow \bar{\mathcal{R}}_0 > 1;\ \bar{\mathcal{R}}_M = 1 \Leftrightarrow \bar{\mathcal{R}}_0 = 1;\ \bar{\mathcal{R}}_M < 1 \Leftrightarrow \bar{\mathcal{R}}_0 < 1. \tag{8}$$

Consider equation $\bar{g}(I_h) = 0$, where

$$\bar{g}(I_h) = \bar{Q}_2 I_h^2 + \bar{Q}_1 I_h + \bar{Q}_0, \tag{9}$$

with

$$\bar{Q}_2 = \alpha\frac{b\beta_v}{N_h}(r + d_h) + \frac{b^2\beta_h\beta_v}{N_h^2}N_v\alpha,\ \ \bar{Q}_0 = d_v(r + d_h + \delta)(1 - \bar{\mathcal{R}}_0),$$
$$\bar{Q}_1 = \alpha d_v(r + d_h + \delta)(1 - \bar{\mathcal{R}}_0) - \delta\alpha d_v + \frac{b\beta_v}{N_h}(r + d_h + \delta) + \frac{b^2\beta_h\beta_v}{N_h^2}N_v.$$

Accordingly, when $\alpha > 0$ and $\bar{Q}_1^2 - 4\bar{Q}_0\bar{Q}_2 \geq 0$, denote

$$\bar{I}_{h1} = \frac{-\bar{Q}_1 - \sqrt{\bar{Q}_1^2 - 4\bar{Q}_0\bar{Q}_2}}{2\bar{Q}_2},\ \ \bar{I}_{h2} = \frac{-\bar{Q}_1 + \sqrt{\bar{Q}_1^2 - 4\bar{Q}_0\bar{Q}_2}}{2\bar{Q}_2}.$$

Define $\bar{E}_1 = (\bar{I}_{h1}, \bar{I}_{v1})^{\mathrm{T}}$ and $\bar{E}_2 = (\bar{I}_{h2}, \bar{I}_{v2})^{\mathrm{T}}$ with $\bar{I}_{vi} = \frac{b\beta_v N_v \bar{I}_{hi}}{b\beta_v \bar{I}_{hi} + d_v N_h}, i = 1, 2$. Then $\bar{E}_1$ and $\bar{E}_2$ are candidates for the endemic equilibrium of system (6).

In addition, denote

$$\bar{\alpha}_0 = \frac{b\beta_v N_h(r+d_h+\delta)+b^2\beta_h\beta_v N_v}{\delta d_v N_h^2},$$
$$\bar{P}_0 = 1+\frac{-\delta\alpha d_v N_h^2+b\beta_v N_h(r+d_h+\delta)+b^2\beta_h\beta_v N_v}{\alpha d_v(r+d_h+\delta)N_h^2}.$$

For $\alpha > \bar{\alpha}_0$, define

$$\bar{\mathcal{R}}_0^+ = 1-\frac{1}{\alpha d_v(r+d_h+\delta)}\left(\sqrt{\alpha d_v\delta-\frac{b\beta_v}{N_h}\delta}-\sqrt{\frac{b\beta_v}{N_h}(r+d_h)+\frac{b^2\beta_h\beta_v}{N_h^2}N_v}\right)^2,$$
$$\bar{\mathcal{R}}_0^- = 1-\frac{1}{\alpha d_v(r+d_h+\delta)}\left(\sqrt{\alpha d_v\delta-\frac{b\beta_v}{N_h}\delta}+\sqrt{\frac{b\beta_v}{N_h}(r+d_h)+\frac{b^2\beta_h\beta_v}{N_h^2}N_v}\right)^2.$$

Through calculations, when $\alpha > \bar{\alpha}_0$, one arrives

$$\max\{0,\ \bar{\mathcal{R}}_0^-\} < \bar{P}_0 < \bar{\mathcal{R}}_0^+ < 1.$$

Theorem 2 *When $\alpha > 0$, we have*

(i) *For $\bar{\mathcal{R}}_0 > 1$, system (6) has a unique endemic equilibrium $\bar{E}_2$;*
(ii) *For $\bar{\mathcal{R}}_0^+ < \bar{\mathcal{R}}_0 < 1$ and $\alpha > \bar{\alpha}_0$, system (6) has two endemic equilibria $\bar{E}_1$ and $\bar{E}_2$;*
(iii) *For $\bar{\mathcal{R}}_0 = 1$ and $\alpha > \bar{\alpha}_0$, system (6) has a unique endemic equilibrium $\bar{E}_2$;*
(iv) *For $\bar{\mathcal{R}}_0 = \bar{\mathcal{R}}_0^+$ and $\alpha > \bar{\alpha}_0$, two endemic equilibria of system (6) coalesce at $\breve{E}$;*
(v) *For $\bar{\mathcal{R}}_0 < \bar{\mathcal{R}}_0^+$ and $\alpha > \bar{\alpha}_0$, system (6) has no endemic equilibrium;*
(vi) *For $\bar{\mathcal{R}}_0 \le 1$ and $\alpha \le \bar{\alpha}_0$, system (6) has no endemic equilibrium.*

Proof of Theorem 2 is given in Appendix A.

Theorem 3 *When $\alpha = 0$, if $\bar{\mathcal{R}}_0 > 1$, then system (6) admits a unique endemic equilibrium $\bar{E}_3 = (\bar{I}_{h3}, \bar{I}_{v3})^{\mathrm{T}}$; otherwise, system (6) admits no endemic equilibrium, where*

$$\bar{I}_{h3} = -\frac{\bar{Q}_0}{\bar{Q}_1},\ \bar{I}_{v3} = \frac{b\beta_v\bar{I}_{h3}N_v}{b\beta_v\bar{I}_{h3}+d_vN_h}.$$

3.2 Stability and bifurcation analysis for non-spatial system

The part is devoted to exploring the dynamics of non-spatial system

$$\begin{cases}\dfrac{\mathrm{d}I_h}{\mathrm{d}t} = b\beta_h\dfrac{I_v}{N_h}(N_h-I_h)-\dfrac{\delta I_h}{1+\alpha I_h}-rI_h-d_hI_h,\\ \dfrac{\mathrm{d}I_v}{\mathrm{d}t} = b\beta_v\dfrac{I_h}{N_h}(N_v-I_v)-d_vI_v.\end{cases} \tag{10}$$

Clearly, for system (10), $\bar{\Gamma} = \{(I_h, I_v)^{\mathrm{T}} \big| 0 \le I_h \le N_h,\ 0 \le I_v \le N_v\}$ is positively invariant.

3.2.1 Stability of equilibria

Let any equilibrium of system (10) be $\bar{E}^* = (\bar{I}_h^*, \bar{I}_v^*)^{\mathrm{T}}$. Take $\bar{y} = (\bar{y}_1, \bar{y}_2)^{\mathrm{T}}$ with $\bar{y}_1 = I_h - \bar{I}_h^*$, $\bar{y}_2 = I_v - \bar{I}_v^*$. Linearizing system (10) at equilibrium $\bar{E}^*$, one has

$$\frac{\mathrm{d}\bar{y}}{\mathrm{d}t} = J(\bar{E}^*)\bar{y}, \tag{11}$$

where

$$J(\bar{E}^*) = \begin{pmatrix} -\bar{\beta}_h \bar{I}_v^* - d_h - r - \frac{\delta}{(1+\alpha \bar{I}_h^*)^2} & \bar{\beta}_h(N_h - \bar{I}_h^*) \\ \bar{\beta}_v(N_v - I_v^*) & -\bar{\beta}_v \bar{I}_h^* - d_v \end{pmatrix}$$

with

$$\bar{\beta}_h = \frac{b\beta_h}{N_h},\ \bar{\beta}_v = \frac{b\beta_v}{N_h}.$$

The characteristic equation associated with $\bar{E}^*$ is

$$\lambda^2 + \bar{A}_0(\bar{E}^*)\lambda + \bar{B}_0(\bar{E}^*) = 0, \tag{12}$$

in which

$$\bar{A}_0(\bar{E}^*) = \bar{\beta}_h \bar{I}_v^* + r + d_h + \frac{\delta}{(1+\alpha \bar{I}_h^*)^2} + \bar{\beta}_v \bar{I}_h^* + d_v,$$

$$\bar{B}_0(\bar{E}^*) = \left(\bar{\beta}_h \bar{I}_v^* + r + d_h + \frac{\delta}{(1+\alpha \bar{I}_h^*)^2}\right)(\bar{\beta}_v \bar{I}_h^* + d_v) - \bar{\beta}_h \bar{\beta}_v (N_h - \bar{I}_h^*)(N_v - \bar{I}_v^*).$$

Note that

$$\bar{B}_0(\bar{E}_k) = \frac{\bar{I}_{hk}}{1+\alpha \bar{I}_{hk}} \bar{g}'(\bar{I}_{hk}),\ k = 1, 2, \tag{13}$$

in which $\bar{g}(I_h)$ is definded in (9). Moreover, one has that $\bar{g}'(\bar{I}_{h1}) < 0$ and $\bar{g}'(\bar{I}_{h2}) > 0$. Hence, $\bar{B}_0(\bar{E}_1) < 0$ and $\bar{B}_0(\bar{E}_2) > 0$. Besides, $\bar{B}_0(\bar{E}_0) = (r + d_h + \delta)d_v(1 - \bar{\mathcal{R}}_0)$.

Theorem 4 *Consider system (10) with $\alpha > 0$.*

(i) *$\bar{E}_0$ is locally asymptotically stable if $\bar{\mathcal{R}}_0 < 1$ and unstable if $\bar{\mathcal{R}}_0 > 1$. Moreover, $\bar{E}_0$ is globally asymptotically stable in $\bar{\Gamma}$ when it is a unique equilibrium for $\bar{\mathcal{R}}_0 < 1$.*

(ii) *$\bar{E}_1$ is unstable whenever it exists.*

(iii) *When $\bar{E}_2$ exists, $\bar{E}_2$ is locally asymptotically stable. Moreover, it is globally asymptotically stable in $\bar{\Gamma} \setminus \{\bar{E}_0\}$ if $\bar{\mathcal{R}}_0 > 1$.*

Proof of Theorem 4 is given in Appendix B.

Corollary 1 *Consider system (10) with* $\alpha = 0$.

(i) $\bar{E}_0$ *is globally asymptotically stable in* $\bar{\Gamma}$ *if* $\bar{\mathcal{R}}_0 < 1$ *and unstable if* $\bar{\mathcal{R}}_0 > 1$.
(ii) *If* $\bar{\mathcal{R}}_0 > 1$, *then* $\bar{E}_3$ *is globally asymptotically stable in* $\bar{\Gamma} \setminus \{\bar{E}_0\}$.

Remark 1 (i) Based on the relationship between $\bar{\mathcal{R}}_M$ and $\bar{\mathcal{R}}_0$ (8) and the biological significance of $\bar{\mathcal{R}}_M$, $\bar{\mathcal{R}}_M$ is used to explain the biological significance of dynamics. Theorem 4 gives the stability of equilibria for system (10) in the presence of the delayed effect for treatment. Biologically, when the basic reproduction number $\bar{\mathcal{R}}_M$ is small (i.e., $\bar{\mathcal{R}}_M < \bar{\mathcal{R}}_M^+ = \sqrt{\bar{\mathcal{R}}_0^+}$) or the delayed effect for treatment is weak (i.e., $\alpha \leq \bar{\alpha}_0$), malaria can be eliminated. And when $\bar{\mathcal{R}}_M$ increases above $\bar{\mathcal{R}}_M^+$ but below one, and the treatment delay effect is strong (i.e., $\alpha > \bar{\alpha}_0$), system (10) allows for bistability. That is, the stable DFE $\bar{E}_0$ coexist with a stable endemic equilibrium $\bar{E}_2$. Under this case, if the initial infection level is different, then malaria may have different epidemic trends, and whether malaria can break out depends on the initial infection level. When $\bar{\mathcal{R}}_M$ is further increased to more than one, no matter whether the treatment delay effect is strong or weak, malaria breaks out.
(ii) Corollary 1 shows the stability of equilibria for system (10) in the absence of the delayed effect for treatment. In the case, malaria can be eliminated if $\bar{\mathcal{R}}_M$ is less than one. As $\bar{\mathcal{R}}_M$ is greater than one, malaria is prevalent.
(iii) Combining Theorem 4 and Corollary 1, if $\bar{\mathcal{R}}_M$ is less than $\bar{\mathcal{R}}_M^+$ (or greater than one), then the disease is extinct (or exists) regardless of including the delayed effect for treatment. However, as $\bar{\mathcal{R}}_M$ is greater than $\bar{\mathcal{R}}_M^+$ and less than one, the existence of this effect makes the disease not necessarily extinct, depending on the strength of this effect and the initial level of infection. Accordingly, the delayed effect for treatment is the fundamental reason for the occurrence of bistability in system (10).

3.2.2 Backward bifurcation

By Theorem 2, when $\bar{\mathcal{R}}_0^+ < \bar{\mathcal{R}}_0 < 1$ and $\alpha > \bar{\alpha}_0$, system (10) has two epidemic equilibria. Consequently, backward bifurcation may occur. In view of Zhao et al. (2020), one arrives the following outcome.

Theorem 5 *System (10) undergoes, at* $\bar{\mathcal{R}}_0 = 1$, *a backward bifurcation for* $\alpha > \bar{\alpha}_1$, *and a forward bifurcation for* $\alpha < \bar{\alpha}_1$, *where*

$$\bar{\alpha}_1 = \frac{d_v + \bar{\beta}_v N_h}{\bar{\delta}_1 N_h d_v}(r + d_h + \bar{\delta}_1), \tag{14}$$

in which $\bar{\delta}_1 = \frac{\bar{\beta}_h \bar{\beta}_v N_h N_v}{d_v} - r - d_h$.

Proof of Theorem 5 is given in Appendix C.

Remark 2 (i) Biologically, $\alpha < \bar{\alpha}_1$ indicates weak delayed effect for treatment. Under the scenario, the basic reproduction number $\bar{\mathcal{R}}_M = 1$ regards as threshold quantity to determine whether malaria will eventually die out or not. Conversely, $\alpha > \bar{\alpha}_1$ means

that such effect is strong. Under the situation, unless $\bar{\mathcal{R}}_M$ is reduced below a new threshold $\bar{\mathcal{R}}_M^+$, it may not be possible to eliminate disease by reducing $\bar{\mathcal{R}}_M$ below one. This is because when $\bar{\mathcal{R}}_M$ is greater than $\bar{\mathcal{R}}_M^+$ and less than one, system (10) shows bistability. From a biological point of view, if there is a difference in the initial infection level, then there may be different epidemic trends, and the disease extinction and outbreak depend on the initial infection level. Besides, if there is no delayed effect for treatment, then system (10) only exhibits forward bifurcation and does not exhibit backward bifurcation. This indicates that the delayed effect for treatment is the fundamental cause of backward bifurcation in system (10). Neglecting the delayed effect for treatment may underestimate the risk of malaria.
(ii) With the aid of (12), $\bar{A}_0(\bar{E}^*) > 0$. It infers that system (6) does not undergo Hopf bifurcation and Bogdanov–Takens bifurcation at $\bar{E}^*$. Hence, when $\mathcal{R}_0 < 1$, the prevalence level of malaria is mainly extinction or bistability, and does not involve periodic cycle.

3.3 Stability of equilibria for system (6)

This part aims to investigate stability of equilibria for system (6). Denote $\mathbb{N}_0 = \{0, 1, 2, \cdots\}$. The linearization of system (6) at equilibrium $\bar{E}^*$ reads as

$$\frac{\partial \bar{y}}{\partial t} = \begin{pmatrix} d_1 & 0 \\ 0 & d_2 \end{pmatrix} \Delta \bar{y} + J(\bar{E}^*)\bar{y}.$$

Accordingly, the characteristic equation associated with $\bar{E}^*$ is

$$\lambda^2 + \bar{A}^{(i)}(\bar{E}^*)\lambda + \bar{B}^{(i)}(\bar{E}^*) = 0, \ i \in \mathbb{N}_0, \tag{15}$$

in which

$$\begin{aligned}
\bar{A}^{(i)}(\bar{E}^*) &= (d_1 + d_2)u_i + \bar{\beta}_h \bar{I}_v^* + r + d_h + \frac{\delta}{(1+\alpha \bar{I}_h^*)^2} + \bar{\beta}_v \bar{I}_h^* + d_v, \\
\bar{B}^{(i)}(\bar{E}^*) &= d_1 d_2 u_i^2 + \left(d_1(\bar{\beta}_v \bar{I}_h^* + d_v) + d_2 \left(\bar{\beta}_h \bar{I}_v^* + r + d_h + \frac{\delta}{(1+\alpha \bar{I}_h^*)^2} \right) \right) u_i \\
&\quad + \left(\bar{\beta}_h \bar{I}_v^* + r + d_h + \frac{\delta}{(1+\alpha \bar{I}_h^*)^2} \right) (\bar{\beta}_v \bar{I}_h^* + d_v) \\
&\quad - \bar{\beta}_h \bar{\beta}_v (N_h - \bar{I}_h^*)(N_v - \bar{I}_v^*),
\end{aligned}$$

where $u_i = \frac{i^2}{l^2}$ is the eigenvalues of $-\Delta$ under homogeneous Neumann boundary condition.

Theorem 6 *For system (6) with $\alpha > 0$, we acquire*

(i) *$\bar{E}_0$ is locally asymptotically stable if $\bar{\mathcal{R}}_0 < 1$ and unstable if $\bar{\mathcal{R}}_0 > 1$;*
(ii) *$\bar{E}_1$ is unstable whenever it exists;*

(iii) *If $\bar{E}_2$ exists, then it is locally asymptotically stable.*

Corollary 2 *Consider system (6) with $\alpha = 0$.*

(i) *$\bar{E}_0$ is locally asymptotically stable if $\bar{\mathcal{R}}_0 < 1$ and unstable if $\bar{\mathcal{R}}_0 > 1$.*
(ii) *If $\bar{\mathcal{R}}_0 > 1$, then $\bar{E}_3$ is locally asymptotically stable.*

Remark 3 (i) Considering the delayed effect for treatment, Theorem 6 provides the stability of equilibria when both humans and mosquitoes have dispersal. Biologically, when the basic reproduction number $\bar{\mathcal{R}}_M$ is less than one, if the initial infection level is low (i.e., near the DFE $\bar{E}_0$), then malaria dies out. In addition, when the endemic equilibrium $\bar{E}_2$ exists, as the initial infection level is near $\bar{E}_2$, malaria is prevalent. Specifically, according to Theorem 2, when $\bar{\mathcal{R}}_M^+ < \bar{\mathcal{R}}_M < 1$ and $\alpha > \bar{\alpha}_0$, system (6) may exhibit bistability. The epidemic trend of the disease at this time is closely related to the initial infection level. When the initial infection level is near $\bar{E}_0$ (or $\bar{E}_2$), the disease becomes extinct (or erupts).
(ii) Excluding the delayed effect for treatment, Corollary 2 gives the stability of equilibria when both human and mosquito populations have spread. Biologically, as the initial infection level is low, malaria is eliminated if $\bar{\mathcal{R}}_M$ is less than one. When $\bar{\mathcal{R}}_M$ is greater than one, if the initial infection level is near $\bar{E}_3$, then the disease breaks out.
(iii) Theorem 6 and Corollary 2 suggest that, when $\bar{\mathcal{R}}_M$ is greater than one and the initial infection level is near the endemic equilibrium, the delayed effect for treatment has negligible impact on the evolutionary outcome of malaria. However, when $\bar{\mathcal{R}}_M$ is less than one, the presence of this effect may increase the possibility of malaria outbreak since $\bar{E}_2$ is locally asymptotically stable. Besides, note that system (6) with $\alpha \geq 0$ does not exhibit complex dynamical behaviors, such as Turing instability, Hopf bifurcation and Turing–Hopf bifurcation. Biologically, regardless of whether the delayed effect for treatment, the malaria may eventually stabilize at a constant level, which means that malaria may not exhibit uneven distribution in space or periodic fluctuation in time.

4 Dynamics analysis for system (5) and its non-spatial system

In this section, we offer the existence of equilibria, and then analyze the stability and bifurcation of system (5) and its non-spatial system.

In view of Lou and Zhao (2011), Shi and Zhao (2021), Shi et al. (2021), one arrives the following result.

Theorem 7 *System (5) admits a unique global classical solution $(I_h, R_h, I_v)^{\mathrm{T}}$ for $t \geq 0$, $x \in \bar{\Omega}$. Further, if $I_h^0(x) \not\equiv 0$, $R_h^0(x) \not\equiv 0$, $I_v^0(x) \not\equiv 0$, then $I_h > 0$, $R_h > 0$, $I_v > 0$ for $t > 0$, $x \in \bar{\Omega}$.*

4.1 Existence of equilibria

Obviously, system (5) always has a DFE $E_0 = (0, 0, 0)^{\mathrm{T}}$. According to Wang and Zhao (2012), define the basic reproduction number

$$\mathcal{R}_M = \sqrt{\mathcal{R}_{I_h} + \mathcal{R}_{R_h}}, \tag{16}$$

where

$$\mathcal{R}_{I_h} = \frac{b\beta_v N_v}{N_h} \cdot \frac{1}{r + d_h + \delta} \cdot b\beta_h \cdot \frac{1}{d_v},$$
$$\mathcal{R}_{R_h} = \frac{r}{r + d_h + \delta} \cdot \frac{b\theta\beta_v N_v}{N_h} \cdot \frac{1}{v + d_h} \cdot b\beta_h \cdot \frac{1}{d_v}.$$

The interpretation of $\mathcal{R}_M$ is similar to that of $\bar{\mathcal{R}}_M$. Note that $\mathcal{R}_M$ and the delayed effect for treatment are irrelevant, because the delayed effect for treatment is only present when the infected persons are more numerous.

Remark 4 (i) In view of (7) and (16), one has $\bar{\mathcal{R}}_M < \mathcal{R}_M$. The reason is that the infectivity of natural recovery individuals is neglected in the modeling of system (10). This may lead to $\bar{\mathcal{R}}_M < 1$ and $\mathcal{R}_M > 1$.

(ii) According to (16), $\mathcal{R}_{I_h}$ monotonically decreases with respect to r, while $\mathcal{R}_{R_h}$ monotonically increases with respect to r. The inconsistency between the monotonicity of $\mathcal{R}_{I_h}$ and $\mathcal{R}_{R_h}$ makes monotonicity of the basic reproduction number $\mathcal{R}_M$ about r variable. Recall that for system (6), the basic reproduction number $\bar{\mathcal{R}}_M$ is monotonically decreasing with respect to r. Thereby, there is significant difference between monotonicity of $\bar{\mathcal{R}}_M$ and $\mathcal{R}_M$ about r.

For brevity, denote $\mathcal{R}_0 = (\mathcal{R}_M)^2$. One has that

$$\mathcal{R}_M > 1 \Leftrightarrow \mathcal{R}_0 > 1; \quad \mathcal{R}_M = 1 \Leftrightarrow \mathcal{R}_0 = 1; \quad \mathcal{R}_M < 1 \Leftrightarrow \mathcal{R}_0 < 1. \tag{17}$$

Define $\alpha_1 = \frac{r}{v + d_h}$. As similar to the previous analysis, consider $g(I_h) = 0$, in which

$$g(I_h) = Q_2 I_h^2 + Q_1 I_h + Q_0, \tag{18}$$

with

$$Q_2 = \alpha \frac{b\beta_v}{N_h}(r + d_h)(1 + \theta\alpha_1) + \frac{b^2\beta_h\beta_v}{N_h^2} N_v \alpha (1 + \theta\alpha_1)(1 + \alpha_1),$$
$$Q_0 = d_v(r + d_h + \delta)(1 - \mathcal{R}_0),$$
$$Q_1 = \alpha d_v(r + d_h + \delta)(1 - \mathcal{R}_0) - \delta\alpha d_v + \frac{b\beta_v}{N_h}(r + d_h + \delta)(1 + \theta\alpha_1)$$
$$+ \frac{b^2\beta_h\beta_v}{N_h^2} N_v (1 + \theta\alpha_1)(1 + \alpha_1).$$

For $\alpha > 0$ and $Q_1^2 - 4Q_0Q_2 \geq 0$, define

$$I_{h1} = \frac{-Q_1 - \sqrt{Q_1^2 - 4Q_0Q_2}}{2Q_2},\ I_{h2} = \frac{-Q_1 + \sqrt{Q_1^2 - 4Q_0Q_2}}{2Q_2}.$$

Denote $E_1 = (I_{h1}, R_{h1}, I_{v1})^{\mathrm{T}}$ and $E_2 = (I_{h2}, R_{h2}, I_{v2})^{\mathrm{T}}$, in which

$$R_{hi} = \alpha_1 I_{hi},\ I_{vi} = \frac{b\beta_v(I_{hi} + \theta R_{hi})N_v}{b\beta_v(I_{hi} + \theta R_{hi}) + d_v N_h},\ i = 1,\ 2.$$

Thereby, E_1 and E_2 are candidates for the endemic equilibrium of system (5).

For brevity, introduce

$$\alpha_0 = \frac{b\beta_v N_h(r + d_h + \delta)(1 + \theta\alpha_1) + b^2\beta_h\beta_v N_v(1 + \theta\alpha_1)(1 + \alpha_1)}{\delta d_v N_h^2},$$
$$P_0 = 1 + \frac{-\delta\alpha d_v N_h^2 + b\beta_v N_h(r + d_h + \delta)(1 + \theta\alpha_1) + b^2 N_v\beta_h\beta_v(1 + \theta\alpha_1)(1 + \alpha_1)}{\alpha d_v(r + d_h + \delta)N_h^2}.$$

For $\alpha > \alpha_0$, define

$$\mathcal{R}_0^+ = 1 - \frac{\left(\sqrt{m_1} - \sqrt{m_2}\right)^2}{\alpha d_v(r + d_h + \delta)},\ \mathcal{R}_0^- = 1 - \frac{\left(\sqrt{m_1} + \sqrt{m_2}\right)^2}{\alpha d_v(r + d_h + \delta)},$$

with

$$m_1 = \alpha d_v\delta - \frac{b\beta_v}{N_h}\delta(1 + \theta\alpha_1),$$
$$m_2 = \frac{b\beta_v}{N_h}(r + d_h)(1 + \theta\alpha_1) + \frac{b^2\beta_h\beta_v}{N_h^2}N_v(1 + \theta\alpha_1)(1 + \alpha_1).$$

When $\alpha > \alpha_0$, one can obtain

$$\max\{0,\ \mathcal{R}_0^-\} < P_0 < \mathcal{R}_0^+ < 1.$$

Theorem 8 *With $\alpha > 0$, the following conclusions are valid.*

(i) *When $\mathcal{R}_0 > 1$, system (5) possesses a unique endemic equilibrium E_2.*
(ii) *When $\mathcal{R}_0^+ < \mathcal{R}_0 < 1$ and $\alpha > \alpha_0$, system (5) possesses two endemic equilibria E_1 and E_2.*
(iii) *When $\mathcal{R}_0 = 1$ and $\alpha > \alpha_0$, system (5) possesses a unique endemic equilibrium E_2.*
(iv) *When $\mathcal{R}_0 = \mathcal{R}_0^+$ and $\alpha > \alpha_0$, two endemic equilibria of system (5) coalesce at $\hat{E}$.*
(v) *When $\mathcal{R}_0 < \mathcal{R}_0^+$ and $\alpha > \alpha_0$, system (5) possesses no endemic equilibrium.*
(vi) *When $\mathcal{R}_0 \leq 1$ and $\alpha \leq \alpha_0$, system (5) possesses no endemic equilibrium.*

Theorem 9 *For $\alpha = 0$, if $\mathcal{R}_0 > 1$, then system (5) admits a unique endemic equilibrium $E_3 = (I_{h3}, R_{h3}, I_{v3})^{\mathrm{T}}$; otherwise, system (5) admits no endemic equilibrium, where*

$$I_{h3} = -\frac{Q_0}{Q_1},\ R_{h3} = -\alpha_1 \frac{Q_0}{Q_1},\ I_{v3} = \frac{b\beta_v(I_{h3} + \theta R_{h3})N_v}{b\beta_v(I_{h3} + \theta R_{h3}) + d_v N_h}.$$

4.2 Stability and bifurcation analysis for non-spatial system

This part focuses on dynamics analysis for non-spatial system

$$\begin{cases} \dfrac{\mathrm{d}I_h}{\mathrm{d}t} = b\beta_h \dfrac{I_v}{N_h}(N_h - I_h - R_h) - \dfrac{\delta I_h}{1 + \alpha I_h} - rI_h - d_h I_h, \\ \dfrac{\mathrm{d}R_h}{\mathrm{d}t} = rI_h - d_h R_h - vR_h, \\ \dfrac{\mathrm{d}I_v}{\mathrm{d}t} = b\beta_v \dfrac{I_h + \theta R_h}{N_h}(N_v - I_v) - d_v I_v. \end{cases} \tag{19}$$

Obviously, for system (19), $\Gamma = \{(I_h, R_h, I_v)^{\mathrm{T}} | 0 \le I_h \le N_h,\ 0 \le R_h \le N_h,\ 0 \le I_v \le N_v\}$ is positively invariant.

4.2.1 Stability of equilibria

Let any equilibrium be $E^* = (I_h^*, R_h^*, I_v^*)^{\mathrm{T}}$. Set $y = (y_1, y_2, y_3)^{\mathrm{T}}$ with $y_1 = I_h - I_h^*$, $y_2 = R_h - R_h^*$, $y_3 = I_v - I_v^*$. Linearizing system (19) at equilibrium E^*, we obtain the following linear system

$$\frac{\mathrm{d}y}{\mathrm{d}t} = J(E^*)y,$$

where

$$J(E^*) = \begin{pmatrix} -\bar{\beta}_h I_v^* - d_h - r - \frac{\delta}{(1+\alpha I_h^*)^2} & -\bar{\beta}_h I_v^* & \bar{\beta}_h(N_h - I_h^* - R_h^*) \\ r & -(v + d_h) & 0 \\ \bar{\beta}_v(N_v - I_v^*) & \theta\bar{\beta}_v(N_v - I_v^*) & -\bar{\beta}_v(I_h^* + \theta R_h^*) - d_v \end{pmatrix}.$$

The characteristic equation associated with E^* is

$$\lambda^3 + A_0(E^*)\lambda^2 + B_0(E^*)\lambda + C_0(E^*) = 0, \tag{20}$$

in which

$$
\begin{aligned}
A_0(E^*) &= \bar{\beta}_h I_v^* + r + d_h + \frac{\delta}{(1+\alpha I_h^*)^2} + v + d_h + \bar{\beta}_v(I_h^* + \theta R_h^*) + d_v,\\
B_0(E^*) &= (v+d_h)\left(\bar{\beta}_h I_v^* + r + d_h + \frac{\delta}{(1+\alpha I_h^*)^2}\right)\\
&\quad + (\bar{\beta}_v(I_h^* + \theta R_h^*) + d_v)\left(\bar{\beta}_h I_v^* + r + 2d_h + \frac{\delta}{(1+\alpha I_h^*)^2} + v\right)\\
&\quad + r\bar{\beta}_h I_v^* - \bar{\beta}_h\bar{\beta}_v(N_v - I_v^*)(N_h - I_h^* - R_h^*),\\
C_0(E^*) &= (v+d_h)(\bar{\beta}_v(I_h^* + \theta R_h^*) + d_v)\left(\bar{\beta}_h I_v^* + r + d_h + \frac{\delta}{(1+\alpha I_h^*)^2}\right)\\
&\quad + r\bar{\beta}_h I_v^*(\bar{\beta}_v(I_h^* + \theta R_h^*) + d_v) - r\theta\bar{\beta}_h\bar{\beta}_v(N_v - I_v^*)(N_h - I_h^* - R_h^*)\\
&\quad - \bar{\beta}_h\bar{\beta}_v(v+d_h)(N_v - I_v^*)(N_h - I_h^* - R_h^*).
\end{aligned}
$$

Similar to (13), one acquires

$$
C_0(E_k) = \frac{(v+d_h)I_{hk}}{1+\alpha I_{hk}} g'(I_{hk}),\ k = 1,\ 2, \tag{21}
$$

in which $g(I_h)$ is definded in (18). Further, $g'(I_{h1}) < 0$ and $g'(I_{h2}) > 0$ if $g(I_h) = 0$ admits two real roots I_{h1} and I_{h2}.

Hence, $C_0(E_1) < 0$ and $C_0(E_2) > 0$. In addition, $C_0(E_0) = (v+d_h)d_v(r+d_h+\delta)(1-\mathcal{R}_0)$.

Theorem 10 *For system (19) with $\alpha > 0$,*

(i) *E_0 is locally asymptotically stable if $\mathcal{R}_0 < 1$ and unstable if $\mathcal{R}_0 > 1$; Moreover, E_0 is globally asymptotically stable in Γ when it is a unique equilibrium for $\mathcal{R}_0 < 1$;*
(ii) *E_1 is unstable whenever it exists;*
(iii) *When E_2 exists, E_2 is locally asymptotically stable if $D_0(E_2) > 0$ and unstable if $D_0(E_2) < 0$, where $D_0(E_2) = A_0(E_2)B_0(E_2) - C_0(E_2)$.*

Proof of Theorem 10 is given in Appendix D.

Corollary 3 *For system (19) with $\alpha = 0$,*

(i) *E_0 is globally asymptotically stable in Γ if $\mathcal{R}_0 < 1$ and unstable if $\mathcal{R}_0 > 1$;*
(ii) *If $\mathcal{R}_0 > 1$, then E_3 is globally asymptotically stable in $\Gamma\backslash\{E_0\}$.*

Proof of Corollary 3 is given in Appendix E.

Remark 5 (i) According to the relationship between $\mathcal{R}_M$ and $\mathcal{R}_0$ (17) and the biological significance of $\mathcal{R}_M$, we next use $\mathcal{R}_M$ to explain the biological significance of dynamical behaviors. Theorem 10 provides the stability of equilibria for system (19) in

the presence of the delayed effect for treatment. Biologically, malaria can be eradicated when the basic reproduction number $\mathcal{R}_M$ is small (i.e., $\mathcal{R}_M < \mathcal{R}_M^+ = \sqrt{\mathcal{R}_0^+}$) or the delayed effect for treatment is weak (i.e., $\alpha \leq \alpha_0$). When $\mathcal{R}_M$ is greater than $\mathcal{R}_M^+$ but less than one, and the treatment delay effect is strong (i.e., $\alpha > \alpha_0$), or $\mathcal{R}_M$ is greater than one, if the initial infection level is near the endemic equilibrium E_2, then malaria outbreak may occur. Furthermore, in the first case (i.e., $\mathcal{R}_M^+ < \mathcal{R}_M < 1$, $\alpha > \alpha_0$), system (19) may exhibit bistability. This implies that different initial infection levels may lead to different epidemic trends, and whether malaria becomes extinct or erupts is closely related to the initial infection level.
(ii) The stability of equilibria for system (19) in the absence of the delayed effect for treatment is given in Corollary 3. In the case, the eradication and outbreak of malaria only depend on whether $\mathcal{R}_M$ is less than one or greater than one.
(iii) In view of Theorem 10 and Corollary 3, malaria becomes extinct when $\mathcal{R}_M$ is small (i.e., $\mathcal{R}_M < \mathcal{R}_M^+$), regardless of the existence of the delayed effect for treatment. When $\mathcal{R}_M$ is greater than $\mathcal{R}_M^+$, the presence of this effect may alter the epidemic state of malaria, by affecting the existence and stability of equilibria. Specifically, when $\mathcal{R}_M$ is greater than $\mathcal{R}_M^+$ and less than one, the existence of this effect makes malaria not necessarily extinct, which is related to the strength of this effect and the initial infection level. When $\mathcal{R}_M$ is further greater than one, if the initial infection level is near E_2, then the presence of this effect may change the epidemic pattern of the disease. Accordingly, the delayed effect for treatment plays important role in the complex dynamics of system (19).
(iv) It is worth mentioning that the difference between system (10) and system (19) lies in whether the infectivity of natural recovery humans is ignored. Based on Theorems 2 and 8, the existence of equilibria in system (10) is highly similar to that in system (19), while the stability of the endemic equilibrium $\bar{E}_2$ in system (10) differs from that of the endemic equilibrium E_2 in system (19) (see Theorems 4 and 10). This means that system (10) may misjudge the prevalence pattern of malaria compared to system (19). Therefore, considering the infectivity of natural recovery category can yield more accurate and diverse results.

4.2.2 Backward bifurcation

Thanks to Theorem 8, if $\mathcal{R}_0^+ < \mathcal{R}_0 < 1$ and $\alpha > \alpha_0$, then system (19) possesses two epidemic equilibria. Consequently, backward bifurcation may appear.

Theorem 11 *System* (19) *exhibits, at* $\mathcal{R}_0 = 1$, *a backward bifurcation for* $\alpha > \tilde{\alpha}_1$, *and a forward bifurcation for* $\alpha < \tilde{\alpha}_1$, *where* $\tilde{\alpha}_1 = \frac{d_v(1+\alpha_1)+\tilde{\beta}_v N_h(1+\theta\alpha_1)}{\delta_1 N_h d_v}(r + d_h + \delta_1)$ *with* $\delta_1 = \frac{\tilde{\beta}_h\tilde{\beta}_v N_h N_v}{d_v} + \frac{r\theta\tilde{\beta}_h\tilde{\beta}_v N_h N_v}{d_v(v+d_h)} - r - d_h$.

Remark 6 (i) Biologically, when the delayed effect for treatment is weak (i.e., $\alpha < \tilde{\alpha}_1$), the basic reproduction number $\mathcal{R}_M = 1$ is taken as threshold quantity for malaria elimination. When the delayed effect for treatment is strong (i.e., $\alpha > \tilde{\alpha}_1$), if $\mathcal{R}_M$ is less than one, then the disease outbreak may occur, unless it is further reduced below the new threshold $\mathcal{R}_M^+ = \sqrt{\mathcal{R}_0^+}$. The reason is that bistability may occur when

$\mathcal{R}_M > \mathcal{R}_M^+$, which means that different initial infection levels may lead to different epidemic trends, and whether malaria outbreak depends on the initial infection state. There are methods to reduce $\mathcal{R}_M$, such as investing treatment efforts and decreasing the total density of mosquitoes. Neglecting the delayed effect for treatment results in only forward bifurcation and no backward bifurcation in system (19). This implies that the delayed effect for treatment is the fundamental source of system (19) experiencing backward bifurcation.

(ii) $\bar{\delta}_1 < \delta_1$ infers that with different values of δ, $\bar{\mathcal{R}}_0$ and $\mathcal{R}_0$ are equal to one, respectively. This may lead to different dynamical behaviors. For example, for $\bar{\delta}_1 < \delta < \delta_1$, one arrives $\bar{\mathcal{R}}_0 < 1$ and $\mathcal{R}_0 > 1$. System (10) may underestimate the emergence of malaria.

4.2.3 Hopf bifurcation

We now discuss Hopf bifurcation at E_2 of system (19) and choose α as bifurcation parameter. For certain critical values $\tilde{\alpha}$, if

$$D_0(E_2)(\tilde{\alpha}) = 0, \tag{22}$$

and the transversality condition holds, then Hopf bifurcation can occur. In fact, if there exists $\tilde{\alpha}$ such that (22) is valid, then the characteristic equation (20) takes the following form

$$(\lambda + A_0(E_2)(\tilde{\alpha}))(\lambda^2 + B_0(E_2)(\tilde{\alpha})) = 0,$$

which admits a pair of purely imaginary roots $\lambda_{1,2} = \pm i\sqrt{B_0(E_2)(\tilde{\alpha})}$ and a negative real root $\lambda_3 = -A_0(E_2)(\tilde{\alpha})$.

Next, give the transversal condition. Let

$$\lambda_1 = v_0(\alpha) + i\varpi_0(\alpha),\ \lambda_2 = v_0(\alpha) - i\varpi_0(\alpha),$$

with $v_0(\tilde{\alpha}) = 0$ and $\varpi_0(\tilde{\alpha}) = \sqrt{B_0(E_2)(\tilde{\alpha})}$. Substituting λ_1 into (20) and taking the derivative with respect to α, we have

$$\begin{aligned} Z_1(\alpha)\frac{dv_0(\alpha)}{d\alpha} - Z_2(\alpha)\frac{d\varpi_0(\alpha)}{d\alpha} + Z_3(\alpha) = 0,\\ Z_2(\alpha)\frac{dv_0(\alpha)}{d\alpha} + Z_1(\alpha)\frac{d\varpi_0(\alpha)}{d\alpha} + Z_4(\alpha) = 0, \end{aligned}$$

where

$$\begin{aligned} Z_1(\alpha) &= 3(v_0^2(\alpha) - \varpi_0^2(\alpha)) + 2A_0(E_2)(\alpha)v_0(\alpha) + B_0(E_2)(\alpha),\\ Z_2(\alpha) &= 2A_0(E_2)(\alpha)\varpi_0(\alpha) + 6v_0(\alpha)\varpi_0(\alpha),\\ Z_3(\alpha) &= (C_0(E_2)(\alpha))' + (A_0(E_2)(\alpha))'(v_0^2(\alpha) - \varpi_0^2(\alpha)) + (B_0(E_2)(\alpha))'v_0(\alpha),\\ Z_4(\alpha) &= (B_0(E_2)(\alpha))'\varpi_0(\alpha) + 2(A_0(E_2)(\alpha))'v_0(\alpha)\varpi_0(\alpha). \end{aligned}$$

By some computations, one has $\frac{\mathrm{d}v_0(\alpha)}{\mathrm{d}\alpha}\big|_{\alpha=\tilde{\alpha}} \neq 0$ if $\frac{\mathrm{d}D_0(E_2)(\alpha)}{\mathrm{d}\alpha}\big|_{\alpha=\tilde{\alpha}} \neq 0$.

Theorem 12 *When E_2 exists, if there is $\tilde{\alpha}$ such that $D_0(E_2)(\tilde{\alpha}) = 0$, $\frac{\mathrm{d}D_0(E_2)(\alpha)}{\mathrm{d}\alpha}\big|_{\alpha=\tilde{\alpha}} \neq 0$, then system (19) undergoes Hopf bifurcation at E_2 as $\alpha = \tilde{\alpha}$.*

Remark 7 Based on Corollary 3, Theorems 4 and 12, regardless of whether the basic reproduction number $\mathcal{R}_M$ is less than or greater than one, only when considering both the delayed effect for treatment and the infectivity of natural recovery category can system (19) experience Hopf bifurcation, thereby diversifying the prevalence patterns of malaria. When the extent of the delayed effect for treatment α is near the critical value $\tilde{\alpha}$, system (19) may posses periodic solution. Biologically, malaria exists in the form of periodic outbreaks if the initial infection level is within a certain range.

4.2.4 Bogdanov–Takens bifurcation

The part is dedicated to discuss Bogdanov–Takens bifurcation of system (19) through selecting δ and α as bifurcation parameters. To achieve this, it is assumed that there are $\hat{\delta}$ and $\hat{\alpha}$ that satisfy the following conditions.

(A1) $\mathcal{R}_0 = \mathcal{R}_0^+$ and $\alpha > \alpha_0$.

Exploiting Theorem 8, system (19) possesses a unique endemic equilibrium $\hat{E}$. Further, one arrives $C_0(\hat{E}) = 0$.

(A2) $B_0(\hat{E}) = 0$.

According to (A1) and (A2), $\lambda_{1,2} = 0$ and $\lambda_3 = -A_0(\hat{E})$ are the eigenvalues of $J(\hat{E})$, resulting in that Bogdanov–Takens bifurcation may occur. In view of Wang and Zhao (2022), Zhao et al. (2020), yield the following consequence.

Theorem 13 *Suppose that (A1), (A2), $c_{20} \neq 0$ and $c_{11} + 2b_{20} \neq 0$ hold. Then system (19) undergoes Bogdanov–Takens bifurcation, where b_{20}, c_{11} and c_{20} are defined in Appendix F.*

Remark 8 (i) Under the combined impacts of the delayed effect for treatment and the infectivity of natural recovery humans, system (19) may exhibit Bogdanov–Takens bifurcation when the basic reproduction number $\mathcal{R}_M$ is less than one. From a biological perspective, the prevalence trend of malaria is highly sensitive to treatment recovery rate δ, the extent of the delayed effect for treatment α and the initial infection state. To be specific, the goal of disease control may be achieved by improving δ so that $\mathcal{R}_M$ is less than $\mathcal{R}_M^+$, or timely treating infected individuals so that α is not greater than α_0. However, when $\mathcal{R}_M$ is greater than $\mathcal{R}_M^+$ and the delayed effect for treatment is strong (i.e., $\alpha > \alpha_0$), malaria may present bistability and periodic outbreaks. At this point, the initial infection level determines whether malaria will eventually erupt or not.
(ii) Even if the number of equilibria for system (10) is the same as that for system (19), system (10) may misjudge the epidemic pattern of malaria because of the occurrence of Hopf bifurcation and Bogdanov–Takens bifurcation in system (19). In view of the previous discussion, Table 2 summarizes whether system (10) can replace system (19) in different parameter regions.

Table 2 Substitution results under different parameter regions

Parameter region			Substitution result
$\alpha \le \bar{\alpha}_0$	$\bar{\mathcal{R}}_0 < 1$	$\mathcal{R}_0 < 1$	Yes
		$\mathcal{R}_0 > 1$	No (may underestimate)
	$\bar{\mathcal{R}}_0 > 1$	$\mathcal{R}_0 < 1$	Does not existent
		$\mathcal{R}_0 > 1$	No (may misjudge)
$\bar{\alpha}_0 < \alpha \le \alpha_0$	$\bar{\mathcal{R}}_0 < \bar{\mathcal{R}}_0^+$	$\mathcal{R}_0 < 1$	Yes
		$\mathcal{R}_0 > 1$	No (may underestimate)
	$\bar{\mathcal{R}}_0^+ < \bar{\mathcal{R}}_0 < 1$	$\mathcal{R}_0 < 1$	No (may overestimate)
		$\mathcal{R}_0 > 1$	No (may underestimate)
	$\bar{\mathcal{R}}_0 > 1$	$\mathcal{R}_0 < 1$	Does not existent
		$\mathcal{R}_0 > 1$	No (may misjudge)
$\alpha > \alpha_0$	$\bar{\mathcal{R}}_0 < \bar{\mathcal{R}}_0^+$	$\mathcal{R}_0 < \mathcal{R}_0^+$	Yes
		$\mathcal{R}_0^+ < \mathcal{R}_0 < 1$	No (may underestimate)
		$\mathcal{R}_0 > 1$	No (may underestimate)
	$\bar{\mathcal{R}}_0^+ < \bar{\mathcal{R}}_0 < 1$	$\mathcal{R}_0 < \mathcal{R}_0^+$	No (may overestimate)
		$\mathcal{R}_0^+ < \mathcal{R}_0 < 1$	No (may misjudge)
		$\mathcal{R}_0 > 1$	No (may underestimate)
	$\bar{\mathcal{R}}_0 > 1$	$\mathcal{R}_0 < 1$	Does not existent
		$\mathcal{R}_0 > 1$	No (may misjudge)

4.3 Stability and bifurcation analysis for system (5)

This part analyzes the dynamics of system (5), including stability of equilibria, Turing instability, Hopf bifurcation and Turing–Hopf bifurcation.

4.3.1 Stability of equilibria

Linearizing system (5) at equilibrium E^* yields

$$\frac{\partial y}{\partial t} = D\Delta y + J(E^*)y,$$

where

$$D = \begin{pmatrix} d_1 & 0 & 0 \\ 0 & d_1 & 0 \\ 0 & 0 & d_2 \end{pmatrix}.$$

Accordingly, the characteristic equation is

$$J_i(E^*) = \lambda^3 + A^{(i)}(E^*)\lambda^2 + B^{(i)}(E^*)\lambda + C^{(i)}(E^*) = 0,\ i \in \mathbb{N}_0, \tag{23}$$

in which

$$A^{(i)}(E^*) = A_1(E^*)u_i + A_0(E^*),\ B^{(i)}(E^*) = B_2(E^*)u_i^2 + B_1(E^*)u_i + B_0(E^*),$$
$$C^{(i)}(E^*) = C_3(E^*)u_i^3 + C_2(E^*)u_i^2 + C_1(E^*)u_i + C_0(E^*),$$

where

$$A_1(E^*) = 2d_1 + d_2,\ B_2(E^*) = d_1^2 + 2d_1d_2,\ C_3(E^*) = d_1^2d_2,$$
$$\begin{aligned}B_1(E^*) &= d_1\left(v + d_h + \bar{\beta}_h I_v^* + r + d_h + \frac{\delta}{(1+\alpha I_h^*)^2} + 2\bar{\beta}_v(I_h^* + \theta R_h^*) + 2d_v\right)\\ &\quad + d_2\left(\bar{\beta}_h I_v^* + r + d_h + \frac{\delta}{(1+\alpha I_h^*)^2}\right) + d_2(v + d_h),\end{aligned}$$
$$C_2(E^*) = d_1^2(\bar{\beta}_v(I_h^* + \theta R_h^*) + d_v) + d_1d_2\left(v + 2d_h + \bar{\beta}_h I_v^* + r + \frac{\delta}{(1+\alpha I_h^*)^2}\right),$$
$$\begin{aligned}C_1(E^*) &= d_1\left(\bar{\beta}_h I_v^* + r + 2d_h + \frac{\delta}{(1+\alpha I_h^*)^2} + v\right)(\bar{\beta}_v(I_h^* + \theta R_h^*) + d_v)\\ &\quad + d_2 r\bar{\beta}_h I_v^* + d_2(v + d_h)\left(\bar{\beta}_h I_v^* + r + d_h + \frac{\delta}{(1+\alpha I_h^*)^2}\right)\\ &\quad - d_1\bar{\beta}_h\bar{\beta}_v(N_v - I_v^*)(N_h - I_h^* - R_h^*).\end{aligned}$$

Next, give the stability of E_0 and E_1.

Theorem 14 *Consider system (5) with $\alpha > 0$.*

(i) *E_0 is locally asymptotically stable if $\mathcal{R}_0 < 1$ and unstable if $\mathcal{R}_0 > 1$.*
(ii) *E_1 is unstable whenever it exists.*

Now pay attention to the stability of E_2. Denote $D^{(i)} = A^{(i)}(E_2)B^{(i)}(E_2) - C^{(i)}(E_2)$, $i \in \mathbb{N}_0$. Through calculations, one has

$$D^{(i)} = D_3(E_2)u_i^3 + D_2(E_2)u_i^2 + D_1(E_2)u_i + D_0(E_2),\ i \in \mathbb{N}_0, \tag{24}$$

where

$$\begin{aligned}D_3(E_2) &= d_1d_2(d_1 + d_2) + d_1d_2(2d_1 + d_2) + d_1^2(2d_1 + d_2),\\ D_2(E_2) &= d_1(d_1 + d_2)m_3 + d_2(d_1 + d_2)(v + d_h) + d_1d_2(m_3 + v + d_h)\\ &\quad + d_1(2d_1 + d_2)m_3 + (d_1 + d_2)(2d_1 + d_2)m_4\\ &\quad + d_1d_2\left(m_3 + v + 2d_h + \bar{\beta}_h I_{v2} + \frac{\delta}{(1+\alpha I_{h2})^2}\right) + rd_1d_2\\ &\quad + d_1(2d_1 + d_2)(v + d_h) + d_1^2\left(m_3 + v + d_h + m_4\right),\\ D_0(E_2) &= (m_3 + v + d_h)(v + d_h)m_3 + m_3\left(r + d_h + \frac{\delta}{(1+\alpha I_{h2})^2}\right)\end{aligned}$$

$$
\begin{aligned}
&+m_3m_4\left(m_3+v+2d_h+\bar{\beta}_hI_{v2}+\frac{\delta}{(1+\alpha I_{h2})^2}\right)\\
&+(v+d_h)m_4\left(m_3+v+d_h+m_4\right)+r\bar{\beta}_hI_{v2}\left(m_3+v+d_h+m_4\right)\\
&+r\theta\bar{\beta}_h\bar{\beta}_vm_5(N_v-I_{v2})-\bar{\beta}_h\bar{\beta}_vm_5(N_v-I_{v2})\left(m_3+m_4\right),
\end{aligned}
$$

$$
\begin{aligned}
D_1(E_2)=\;&(d_1+d_2)(v+d_h)m_3+d_1(m_3+v+d_h)m_3+d_2(m_3+v+d_h)(v+d_h)\\
&+(2d_1+d_2)m_3m_4+d_1m_3\left(m_3+v+2d_h+\bar{\beta}_hI_{v2}+\frac{\delta}{(1+\alpha I_{h2})^2}\right)\\
&+d_2m_4\left(m_3+v+2d_h+\bar{\beta}_hI_{v2}+\frac{\delta}{(1+\alpha I_{h2})^2}\right)+rd_1m_3\\
&+rd_2\left(r+d_h+\frac{\delta}{(1+\alpha I_{h2})^2}\right)+(2d_1+d_2)(v+d_h)m_4\\
&+(2d_1+d_2)r\bar{\beta}_hI_{v2}-m_5(d_1+d_2)\bar{\beta}_h\bar{\beta}_v(N_v-I_{v2})\\
&+\left(v+d_h+m_4\right)\left(m_3+v+d_h+m_4\right),
\end{aligned}
\tag{25}
$$

with $m_3=\bar{\beta}_v(I_{h2}+\theta R_{h2})+d_v, m_4=\bar{\beta}_hI_{v2}+r+d_h+\frac{\delta}{(1+\alpha I_{h2})^2}$, $m_5=N_h-I_{h2}-R_{h2}$.

Further, define

$$
\begin{aligned}
&\mathcal{A}_C=(C_2(E_2))^2-3C_1(E_2)C_3(E_2),\ \mathcal{B}_C=C_1(E_2)C_2(E_2)-9C_0(E_2)C_3(E_2),\\
&\mathcal{C}_C=(C_1(E_2))^2-3C_0(E_2)C_2(E_2),\ \Delta_C=\mathcal{B}_C^2-4\mathcal{A}_C\mathcal{C}_C,\\
&\mathcal{A}_D=(D_2(E_2))^2-3D_1(E_2)D_3(E_2),\ \mathcal{B}_D=D_1(E_2)D_2(E_2)-9D_0(E_2)D_3(E_2),\\
&\mathcal{C}_D=(D_1(E_2))^2-3D_0(E_2)D_2(E_2),\ \Delta_D=\mathcal{B}_D^2-4\mathcal{A}_D\mathcal{C}_D.
\end{aligned}
\tag{26}
$$

Theorem 15 *For system (5) with $\alpha>0$, when E_2 exists, if $D_0(E_2)>0$ and the following conditions hold:*

(a) $C_1(E_2)\geq 0$ *or* $C_1(E_2)<0$ *and* $\Delta_C>0$*;*
(b) $D_1(E_2)\geq 0$ *or* $D_1(E_2)<0$ *and* $\Delta_D>0$*,*

then E_2 is locally asymptotically stable.

Proof At E_2, the characteristic equation is

$$
\lambda^3+A^{(i)}(E_2)\lambda^2+B^{(i)}(E_2)\lambda+C^{(i)}(E_2)=0,\ i\in\mathbb{N}_0,
\tag{27}
$$

where $A^{(i)}(E_2)$, $B^{(i)}(E_2)$ and $C^{(i)}(E_2)$ are defined in (23) by replacing E^* with E_2. Note that $A^{(i)}(E_2)>0$, $i\in\mathbb{N}_0$. If $C^{(i)}(E_2)>0$ and $D^{(i)}(E_2)>0$, then $B^{(i)}(E_2)>0$, $i\in\mathbb{N}_0$. Hence, the stability of E_2 is determined by the signs of $C^{(i)}(E_2)$ and $D^{(i)}(E_2)$, $i\in\mathbb{N}_0$.

Apparently, $C_3(E_2)>0$ and $C_2(E_2)>0$. Further, it can be obtained from (21) that $C_0(E_2)>0$. Next, we explore the influence of $C_1(E_2)$ on the sign of $C^{(i)}(E_2)$ for $i\in\mathbb{N}_0\backslash\{0\}$.

Case (I) $C_1(E_2)\geq 0$.

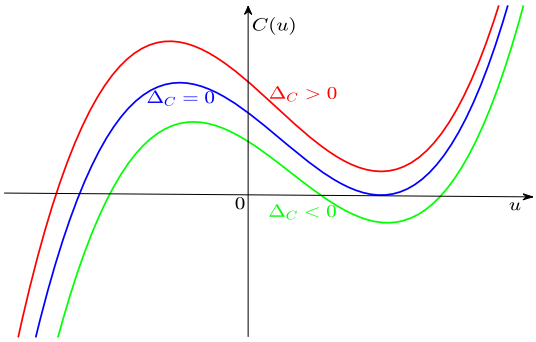

Fig. 2 The distribution of roots for $C(u) = 0$ with $C_1(E_2) < 0$

Obviously, $C^{(i)}(E_2) > 0$, $i \in \mathbb{N}_0\backslash\{0\}$.

Case (II) $C_1(E_2) < 0$.

Define $C(u) = C_3(E_2)u^3 + C_2(E_2)u^2 + C_1(E_2)u + C_0(E_2)$. Then $C'(u) = 3C_3(E_2)u^2 + 2C_2(E_2)u + C_1(E_2)$. Moreover, $C'(u) = 0$ has two different real roots $\bar{u}_1$ and $\bar{u}_2$. Without loss of generality, assume $\bar{u}_1 < \bar{u}_2$. Accordingly, $\bar{u}_1 < 0 < \bar{u}_2$. Notice that $\bar{u}_1$ and $\bar{u}_2$ are inflection points of function $C(u)$. Thus, applying Shengjin's Distinguishing Means (Zhao et al. 2020; Hu et al. 2012), the following results can be acquired:

(i) If $\Delta_C > 0$, then there is no positive root for $C(u) = 0$ (see Fig. 2);
(ii) If $\Delta_C = 0$, then $C(u) = 0$ has three real roots, denoted by $\tilde{u}_1$, $\tilde{u}_2$ and $\tilde{u}_3$, respectively. Without loss of generality, assume $\tilde{u}_1 \le \tilde{u}_2 \le \tilde{u}_3$. Moreover, $\tilde{u}_1 < \bar{u}_1 < 0 < \bar{u}_2 = \tilde{u}_2 = \tilde{u}_3$ (see Fig. 2);
(iii) If $\Delta_C < 0$, then $C(u) = 0$ has three real roots, denoted by $\tilde{u}_1$, $\tilde{u}_2$ and $\tilde{u}_3$, respectively. Suppose $\tilde{u}_1 \le \tilde{u}_2 \le \tilde{u}_3$. Then, $\tilde{u}_1 < \bar{u}_1 < 0 < \tilde{u}_2 < \bar{u}_2 < \tilde{u}_3$ (see Fig. 2).

Hence, when $\Delta_C > 0$, one has $C(u) > 0$ for $u > 0$. Thereby, for $\Delta_C > 0$, we obtain $C^{(i)}(E_2) > 0$, $i \in \mathbb{N}_0\backslash\{0\}$.

Analogously, for $D_0(E_2) > 0$, if the condition (b) holds, then $D^{(i)}(E_2) > 0$, $i \in \mathbb{N}_0\backslash\{0\}$. Consequently, when $D_0(E_2) > 0$ and the conditions (a) and (b) hold, E_2 is locally asymptotically stable. We complete the proof. □

Corollary 4 *For system* (5) *with* $\alpha = 0$,

(i) E_0 *is locally asymptotically stable if* $\mathcal{R}_0 < 1$ *and unstable if* $\mathcal{R}_0 > 1$;
(ii) *If* $\mathcal{R}_0 > 1$, *then* E_3 *is locally asymptotically stable.*

Remark 9 (i) As incorporating the delayed effect for treatment, Theorems 14 and 15 show the stability of equilibria when both humans and mosquitoes have spread. Biologically, when the initial infection level is low (i.e., near the DFE E_0), if the basic reproduction number $\mathcal{R}_M$ is less than one, then malaria becomes extinct.

Besides, based on Theorem 8, as $\mathcal{R}_M^+ < \mathcal{R}_M < 1$ and $\alpha > \alpha_0$ or $\mathcal{R}_M > 1$, if the initial infection level approaches the endemic equilibrium E_2, then malaria outbreak may occur. Note that in the first scenario, bistability may occur, which means that

different initial levels may lead to different evolution trends. To be specific, if the initial infection level is near E_0 (or E_2), malaria becomes extinct (or may erupt).
(ii) Without taking into account the delayed effect for treatment, Corollary 4 gives the stability of equilibria when both human and mosquito populations spread. Biologically, if the initial infection level is low, then the extinction of malaria occurs if $\mathcal{R}_M$ is less than one. When $\mathcal{R}_M$ is greater than one, if the initial infection level is near E_3, then malaria is prevalent.
(iii) Theorems 14 and 15 and Corollary 4 indicate that when $\mathcal{R}_M$ is less than one and the initial infection level is low, the delayed effect for treatment has negligible impact on the evolutionary outcome of malaria. However, it is worth noting that system (5) without this effect does not exhibit complex dynamics, such as Turing instability, Hopf bifurcation and Turing–Hopf bifurcation. Biologically, malaria may eventually stabilize at a constant level, without uneven distribution in space or periodic fluctuation in time. The inclusion of this effect makes both the above complex dynamics and spatiotemporal patterns possible. In particular, when $\mathcal{R}_M^+ < \mathcal{R}_M < 1$ and $\alpha > \alpha_0$, the inclusion of this effect may increase the likelihood of malaria outbreak due to the existence of the endemic equilibria.
(iv) Note that the difference between systems (5) and (6) is whether the infectivity of natural recovery persons is overlooked. In light of the above discussion, the existence of equilibria for system (5) is highly similar to that for system (6) (see Theorems 2 and 8), however the stability of the endemic equilibrium E_2 for system (5) is quite different from that of the endemic equilibrium $\bar{E}_2$ for system (6) (see Theorem 15 and Corollary 4). Specifically, system (6) does not exhibit bifurcation at $\bar{E}_2$, however system (5) may experience bifurcation at E_2. This shows that it is possible to obtain more accurate and rich results by incorporating the infectivity of natural recovery category.

4.3.2 Turing instability

The subsection presents conditions that may lead to Turing instability of E_2 for system (5). For non-spatial system (19), when E_2 exists, E_2 is stable if $D_0(E_2) > 0$. In the following, assume $D_0(E_2) > 0$. If there is a certain $i_0 \in \mathbb{N}_0\backslash\{0\}$ resulting in $C^{(i_0)}(E_2) < 0$, then E_2 of spatial system (5) is unstable and Turing instability occurs.

Theorem 16 *When E_2 exists, if $D_0(E_2) > 0$ and $C^{(i_0)}(E_2) < 0$ for some $i_0 \in \mathbb{N}_0\backslash\{0\}$, then E_2 is Turing unstable.*

Remark 10 When both the infectivity of natural recovery class and the delayed effect for treatment are included, the introduction of diffusion may change the stability of the equilibrium, and both are indispensable. Biologically, the emergence of Turing instability means that when both humans and mosquitoes spread, malaria may not eventually stabilize at a constant equilibrium, but rather exhibit an uneven distribution in space. That is to say, there may be different prevalence levels in different locations.

4.3.3 Hopf bifurcation

With the aid of Song et al. (2016), choose α as bifurcation parameter to explore Hopf bifurcation at E_2 of system (5).

Theorem 17 *When E_2 exists, if there are $i_1 \in \mathbb{N}_0$ and $\bar{\alpha}$ such that $C^{(i_1)}(E_2)(\bar{\alpha}) > 0$, $D^{(i_1)}(E_2)(\bar{\alpha}) = 0$, $\frac{\mathrm{d}D^{(i_1)}(E_2)(\alpha)}{\mathrm{d}\alpha}\big|_{\alpha=\bar{\alpha}} \neq 0$, and for $i \in \mathbb{N}_0\backslash\{i_1\}$, $C^{(i)}(E_2)(\bar{\alpha}) \neq 0$, $D^{(i)}(E_2)(\bar{\alpha}) \neq 0$, then system (5) undergoes Hopf bifurcation at E_2 as $\alpha = \bar{\alpha}$. Further, Hopf bifurcation is spatially homogeneous if $i_1 = 0$ and spatially nonhomogeneous if $i_1 \in \mathbb{N}_0\backslash\{0\}$.*

Remark 11 Only when considering both the infectivity of natural recovery class and the delayed effect for treatment can system (5) undergo Hopf bifurcation. From a biological perspective, the occurrence of the spatially homogeneous Hopf bifurcation in system (5) indicates that malaria may exhibit periodic outbreaks, and the prevalence level does not vary due to regional differences. The appearance of spatially nonhomogeneous Hopf bifurcation in system (5) implies that malaria may not only exhibit periodic outbreaks, but the prevalence level may also vary by region.

4.3.4 Turing–Hopf bifurcation

The part is dedicated to investigate Turing–Hopf bifurcation at E_2 of system (5). To this end, make some hypotheses.

(B1) $D^{(0)}(E_2) = 0$.

By (B1), $J_0(E_2) = 0$ possesses a pair of purely imaginary roots $\pm i\omega_0$ and a negative real root.

(B2) There is a positive integer i^* satisfying that $C^{(i^*)}(E_2) = 0$ and $D^{(i^*)}(E_2) > 0$.

Based on (B2), $J_{i^*}(E_2) = 0$ admits a simple zero root and all other roots having negative real parts.

(B3) For $i \in \mathbb{N}_0\backslash\{0, i^*\}$, $C^{(i)}(E_2) > 0$, $D^{(i)}(E_2) > 0$.

According to (B3), when $i \in \mathbb{N}_0\backslash\{0, i^*\}$, all roots of $J_i(E_2) = 0$ have negative real parts.

Based on the previous analysis, the delayed effect for treatment and the inclusion of natural recovery compartment play significant role in the complex dynamics of system (5). Accordingly, we take the extent of the delayed effects for treatment α and the transformation rate from the infected compartment to the natural recovery compartment (i.e., natural recovery rate) r as bifurcation parameters, and offer transversality conditions. To simplify the discussion, define

$$\Gamma_1 = \left\{(\alpha_{11}, r_{11})\middle|\ D^{(0)}(E_2)(\alpha_{11}, r_{11}) = 0,\ \frac{\mathrm{d}D^{(0)}(E_2)(\alpha, r)}{\mathrm{d}\alpha}\Big|_{(\alpha,r)=(\alpha_{11},r_{11})} \neq 0\right\},$$

$$\Gamma_2 = \left\{(\alpha_{21}, r_{21})\middle|\ C^{(i^*)}(E_2)(\alpha_{21}, r_{21}) = 0,\ D^{(i^*)}(E_2)(\alpha_{21}, r_{21}) > 0,\ \frac{\mathrm{d}C^{(i^*)}(E_2)(\alpha, r)}{\mathrm{d}\alpha}\Big|_{(\alpha,r)=(\alpha_{21},r_{21})} \neq 0\right\}.$$

Suppose that Γ_1 and Γ_2 are non-empty. By the implicit function theorem, in some neighborhood of (α_{11}, r_{11}) $((\alpha_{21}, r_{21}))$, there is a unique continuous function $\alpha =$

$F_1(r)$ ($\alpha = F_2(r)$) satisfying $D^{(0)}(E_2)(F_1(r), r) = 0$ ($C^{(i^*)}(E_2)(F_2(r), r) = 0$). Moreover, let $\lambda_1 = \upsilon_0(\alpha, r) + i\varpi_0(\alpha, r)$, $\lambda_2 = \upsilon_0(\alpha, r) - i\varpi_0(\alpha, r)$ with $\upsilon_0(F_1(r), r) = 0$, $\varpi_0(F_1(r), r) = \sqrt{B^{(0)}(E_2)(F_1(r), r)}$, and $\tilde{\lambda}_1 = \upsilon_1(\alpha, r)$ with $\upsilon_1(F_2(r), r) = 0$. Through calculations, acquire

$$\begin{aligned} \left.\frac{\mathrm{d}\upsilon_0(\alpha, r)}{\mathrm{d}\alpha}\right|_{\alpha=F_1(r)} &= -\frac{2}{\hat{A}}\left.\frac{\mathrm{d}D^{(0)}(E_2)(\alpha, r)}{\mathrm{d}\alpha}\right|_{\alpha=F_1(r)} \neq 0, \\ \left.\frac{\mathrm{d}\upsilon_1(\alpha, r)}{\mathrm{d}\alpha}\right|_{\alpha=F_2(r)} &= -\frac{1}{\hat{B}}\left.\frac{\mathrm{d}C^{(i^*)}(E_2)(\alpha, r)}{\mathrm{d}\alpha}\right|_{\alpha=F_2(r)} \neq 0, \end{aligned} \tag{28}$$

where $\hat{A} = (A^{(0)}(E_2)(F_1(r), r))^2 + B^{(0)}(E_2)(F_1(r), r)$, $\hat{B} = B^{(i^*)}(E_2)(F_2(r), r)$. Hence, the transversality conditions hold. Accordingly, establish the following theorem.

Theorem 18 *When E_2 exists, if there are α^*, r^* and i^* satisfying (B1)–(B3) and transversality conditions, then system (5) exhibits $(i^*, 0)$-mode Turing–Hopf bifurcation at E_2 as $(\alpha, r) = (\alpha^*, r^*)$.*

Applying the method in Song et al. (2016) to system (5), we derive the normal form of Turing–Hopf bifurcation at E_2. More details can be found in Appendix G.

Remark 12 (i) Simultaneously considering the infectivity of natural recovery class and the delayed effect for treatment leads to Turing–Hopf bifurcation in system (5). This indicates that system (5) has rich dynamical behaviors near (α^*, r^*). There may be spatially inhomogeneous steady state, spatially homogeneous and inhomogeneous periodic solutions. From a biological point of view, malaria may exhibit spatiotemporal patterns, such as uneven distribution in space, or periodicity in time and uniform distribution in space, or periodicity in time and uneven distribution in space. In particular, if system (5) admits Turing–Hopf bifurcation as the basic reproduction number $\mathcal{R}_M$ is less than one, then system (5) may exhibit multistability, that is, the DFE E_0 may coexist with spatially inhomogeneous steady state, spatially homogeneous or inhomogeneous periodic solution, respectively. Biologically, different initial infection levels may lead to different epidemic trends, meaning that malaria can become extinct or erupt and exhibit spatiotemporal patterns. In the case, the epidemic pattern of malaria is highly sensitive to the extent of the delayed effect for treatment α, natural recovery rate r, as well as the initial infection level.

(ii) With the aid of Theorems 16-18, for the endemic equilibrium E_2 of system (5), Turing instability, Hopf bifurcation and Turing–Hopf bifurcation may appear. However, for system (6), these dynamic behaviors are not present. The results reveal that the dynamics of system (5) are more complicated and richer than that of system (6). In different parameter areas, whether system (6) can achieve the substitution effect for system (5) is the same as that in Table 2. It is worth mentioning that when comparing non-spatial systems (10) and (19), system (10) may cause misjudgment, as Hopf bifurcation and Bogdanov–Takens bifurcation appear in system (19). At this time, malaria may break out in a periodic pattern. When

comparing spatial systems (6) and (5), system (6) may lead to misjudgment due to Turing instability, Hopf bifurcation and Turing–Hopf bifurcation in system (5). In this case, the disease may stabilize at spatial inhomogeneous steady state, spatially homogeneous or inhomogeneous periodic solution. These results provide new perspective for understanding the influence of the infectivity of natural recovery class on malaria transmission.

5 Numerical simulations

The goal of this part is to carry out numerical simulations, so as to confirm the analytic outcomes and acquire some epidemiological insights.

5.1 Bifurcation diagram and dynamics of system (10)

According to the above discussion, system (10) can exhibit forward bifurcation and backward bifurcation. In this part, we describe the bifurcation diagram, and further discuss the existence and stability of equilibria.

Set

$$\begin{aligned} &N_h = 110,\ N_v = 220,\ b = 0.4,\ \beta_h = 0.02,\ \beta_v = 0.4,\ \theta = 0.1,\\ &r = 0.00144,\ v = 0.0007,\ d_h = \frac{1}{70 \times 365},\ d_v = \frac{1}{25}, \end{aligned} \tag{29}$$

which are adjusted on the basis of Bousema et al. (2010), Wang et al. (2017), Chitnis et al. (2008).

5.1.1 Bifurcation diagram in (α, δ) plane and dynamics for system (10)

Under the above parameters, Fig. 3 presents the bifurcation diagram in (α, δ) plane of system (10). To be specific, $\bar{L}^*$: $\delta = \bar{\delta}_1$ meets $\bar{\mathcal{R}}_0 = 1$. Moreover, $W_1 = (\bar{\alpha}_1, \bar{\delta}_1) \approx (0.047, 0.062)$ divides $\bar{L}^*$ into two parts $\bar{L}^*_-$ $(\alpha < \bar{\alpha}_1)$ and $\bar{L}^*_+$ $(\alpha > \bar{\alpha}_1)$. In view of Theorem 5, system (10) exhibits forward bifurcation and backward bifurcation on $\bar{L}^*_-$ and $\bar{L}^*_+$, respectively. Next, give description of the remaining curves. Curve $\bar{L}_0$ satisfies $\bar{\mathcal{R}}_0 = \bar{\mathcal{R}}_0^+$. Curve $\bar{L}_1$ holds $\alpha = \bar{\alpha}_0$. Further, denote

$$\bar{H}_0 = \bar{H}_{0-1} \cup \bar{H}_{0-2},\ \bar{H}_1 = \{(\alpha, \delta) |\ \bar{\mathcal{R}}_0^+ < \bar{\mathcal{R}}_0 < 1,\ \alpha > \bar{\alpha}_0\},\ \bar{H}_2 = \{(\alpha, \delta) |\ \bar{\mathcal{R}}_0 > 1\},$$

where $\bar{H}_{0-1} = \{(\alpha, \delta) |\ \bar{\mathcal{R}}_0 < 1,\ \alpha \le \bar{\alpha}_0\}$, $\bar{H}_{0-2} = \{(\alpha, \delta) |\ \bar{\mathcal{R}}_0 < \bar{\mathcal{R}}_0^+,\ \alpha > \bar{\alpha}_0\}$. With the aid of Theorem 2 and Theorem 4, the dynamics for system (10) are summarized in Table 3.

5.1.2 Bifurcation diagram in $(\bar{\mathcal{R}}_0, I_h)$ plane and dynamics for system (10)

As $\bar{\mathcal{R}}_0$ a significant indicator, the bifurcation diagram in $(\bar{\mathcal{R}}_0, I_h)$ plane is drawn. To show all bifurcation types in $(\bar{\mathcal{R}}_0, I_h)$ plane, choose $\alpha = 0.04$ and $\alpha = 0.2$.

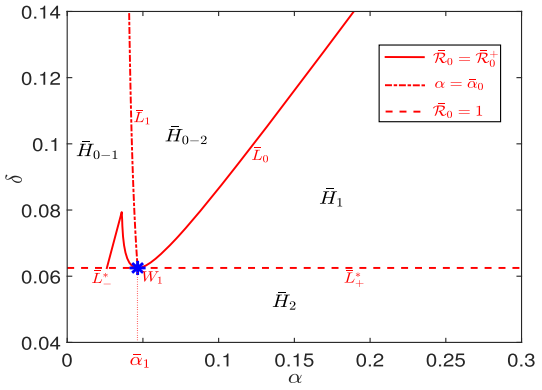

Fig. 3 Bifurcation diagram in (α, δ) plane for system (10)

Table 3 The dynamics of system (10)

	$\bar{E}_0$	$\bar{E}_1$	$\bar{E}_2$
$\bar{H}_0$	LAS	Non	Non
$\bar{H}_1$	LAS	US	LAS
$\bar{H}_2$	US	Non	LAS

For $\alpha = 0.04$, system (10) undergoes forward bifurcation at $\bar{\mathcal{R}}_0 = 1$ (see Fig. 4a). Under the case, system (10) possesses no endemic equilibrium as $\bar{\mathcal{R}}_0 < 1$. The result infers that $\bar{\mathcal{R}}_0 = 1$ serves as threshold quantity for malaria eradication if $\alpha < \bar{\alpha}_1$.

In Fig. 4b, $\alpha = 0.2$ is selected such that $\alpha > \bar{\alpha}_1$. Then backward bifurcation appears at $\bar{\mathcal{R}}_0 = 1$. For $\bar{\mathcal{R}}_0 < 1$, malaria may not be eliminated. This has significance impact on malaria control. As $\bar{\mathcal{R}}_0 < 1$ and $\alpha > \bar{\alpha}_1$, if there are enough infected persons at the initial stage of malaria, then malaria is likely to be prevalent and stabilize at $\bar{E}_2$. Malaria may be eliminated if a few infected individuals are introduced. Accordingly, unless $\bar{\mathcal{R}}_0$ is lower than the new threshold value $\bar{\mathcal{R}}_0^+$, it may not be successful to eliminate disease by reducing $\bar{\mathcal{R}}_0$ below one.

5.2 Bifurcation diagram and dynamics of system (19)

Based on the above discussion, system (19) can undergo Bogdanov–Takens bifurcation. This part is devoted to demonstrating the dynamics of system (19). The parameter values are the same as (29).

5.2.1 Bifurcation diagram in (α, δ) plane and dynamics for system (19)

Using the above parameters, one arrives $BT = (\hat{\alpha}, \hat{\delta}) \approx (0.13, 0.089)$ satisfying $(A1)$, $(A2)$, $c_{20} < 0$ and $c_{11} + 2b_{20} < 0$. From Theorem 13, system (19) exhibits Bogdanov–Takens bifurcation. The bifurcation diagram in (α, δ) plane for system (19) is shown in Fig. 5. More specifically, the blue, green and black solid lines stand for the bifurcation curves of saddle-node (SN), Hopf $(Hopf)$ and homoclinic (Hom),

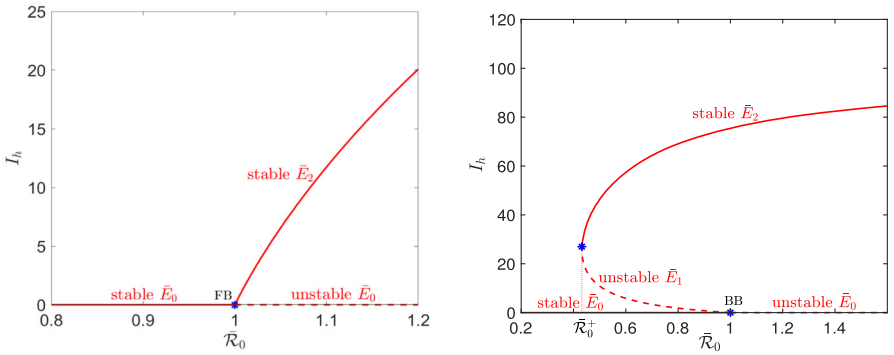

(a) $\alpha = 0.04$ (b) $\alpha = 0.2$

Fig. 4 Bifurcation diagram in $(\bar{\mathcal{R}}_0, I_h)$ plane of system (10) for different α. The solid (dashed) curve stands for stable (unstable) equilibria. FB (BB) represents forward (backward) bifurcation

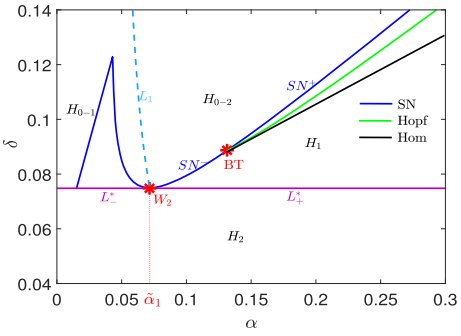

Fig. 5 Bifurcation diagram in (α, δ) plane for system (19)

respectively. BT, the intersection of $Hopf$ and Hom with SN, divides SN into attractive (SN^-) and repulsive (SN^+) saddle-node bifurcation curves.

In addition, curve L^*: $\delta = \delta_1$ is defined by solving $\mathcal{R}_0 = 1$. In light of Theorem 11, L^* is divided into the bifurcation curves of forward (L_-^*) and backward (L_+^*) by $W_2 = (\tilde{\alpha}_1, \delta_1) \approx (0.072, 0.075)$. Curve L_1 meets $\alpha = \alpha_0$. Moreover, introduce

$$H_0 = H_{0-1} \cup H_{0-2},\ H_1 = \{(\alpha, \delta) |\ \mathcal{R}_0^+ < \mathcal{R}_0 < 1,\ \alpha > \alpha_0\},\ H_2 = \{(\alpha, \delta) |\ \mathcal{R}_0 > 1\},$$

in which

$$H_{0-1} = \{(\alpha, \delta) |\ \mathcal{R}_0 < 1,\ \alpha \le \alpha_0\},\ H_{0-2} = \{(\alpha, \delta) |\ \mathcal{R}_0 < \mathcal{R}_0^+,\ \alpha > \alpha_0\}.$$

Based on the outcomes in Sect. 4.2, one arrives the dynamics for system (19) shown in Table 4.

Table 4 The dynamics of system (19)

	E_0	E_1	E_2
H_0	LAS	Non	Non
H_1	LAS	US	Various
H_2	US	Non	LAS

Here LAS, US and Non stand for locally asymptotically stable, unstable and nonexistent, respectively

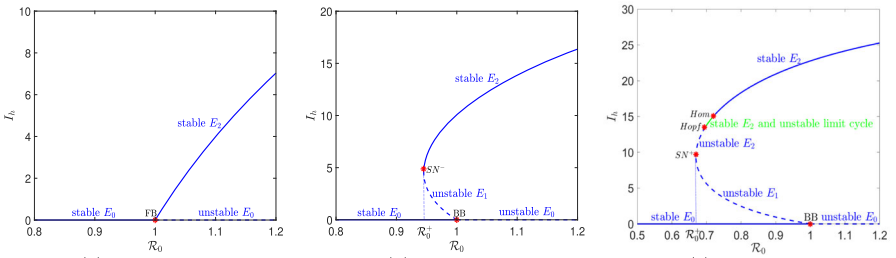

(a) $\alpha = 0.05$ (b) $\alpha = 0.1$ (c) $\alpha = 0.2$

Fig. 6 Bifurcation diagrams in $(\mathcal{R}_0, I_h)$ plane of system (19) for different α. The solid (dashed) curve stands for stable (unstable) equilibria. FB (BB) represents forward (backward) bifurcation

5.2.2 Bifurcation diagram in $(\mathcal{R}_0, I_h)$ plane and dynamics for system (19)

In this part, set $\alpha = 0.05$, $\alpha = 0.1$ and $\alpha = 0.2$ to illustrate all bifurcation diagrams in $(\mathcal{R}_0, I_h)$ plane.

When $\alpha = 0.05$, the forward bifurcation at $\mathcal{R}_0 = 1$ arises, which is illustrated in Fig. 6a. There is no endemic equilibrium if $\mathcal{R}_0 < 1$. This concludes that with weak delayed effect for treatment, $\mathcal{R}_0 = 1$ is used as critical value of disease extinction.

Choose $\alpha = 0.1$ and $\alpha = 0.2$, making $\alpha > \tilde{\alpha}_1$. Saddle-node and backward bifurcations appear (see Fig. 6b, c). Besides, since the appearance of forward Hopf bifurcation, the endemic equilibrium E_2 changes from unstable to stable, and an unstable limit cycle is generated around E_2. Subsequently, it is broken by homoclinic loop (see Fig. 6c). Moreover, Fig. 6b, c indicate that malaria may not die out as $\mathcal{R}_0 < 1$. Biologically, due to strong delayed effect for treatment, there may be bistability in malaria epidemic level if $\mathcal{R}_0^+ < \mathcal{R}_0 < 1$. In the case, the outbreak or extinction of disease is closely related to the initial infection level. As a result, in order to cope with the outbreak of malaria, measures should be implemented to decrease $\mathcal{R}_0$ below $\mathcal{R}_0^+$, otherwise malaria may not be successfully eliminated.

5.3 The comparison between systems (10) and (19)

On the basis of the discussion in Sects. 5.1-5.2, we are in a position to compare dynamics of systems (10) and (19). For convenience, define

$$D_{00} = \bar{H}_0 \cap H_0,\ D_{01} = \bar{H}_0 \cap H_1,\ D_{02} = \bar{H}_0 \cap H_2,\ D_{10} = \bar{H}_1 \cap H_0,$$
$$D_{11} = \bar{H}_1 \cap H_1,\ D_{12} = \bar{H}_1 \cap H_2,\ D_{22} = \bar{H}_2 \cap H_2.$$

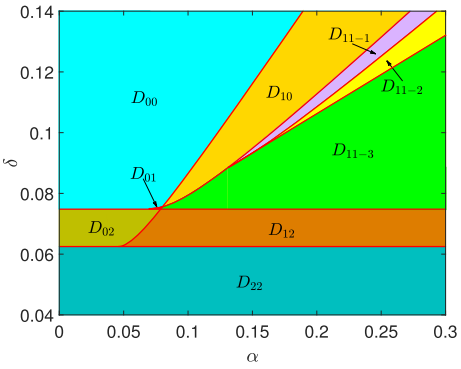

Fig. 7 The subregions of (α, δ) plane

Furthermore, the bifurcation curves of Hopf and homoclinic of system (19) are used as boundary to produce three subsets of D_{11}: D_{11-1}, D_{11-2} and D_{11-3}. Figure 7 shows the distribution of these nine regions in (α, δ) plane. The substitution results of system (10) for (19) in nine regions are summarized in Table 5.

In detail, two systems have zero, one and two endemic equilibria in regions D_{00}, D_{22} and D_{11-3}, respectively. Furthermore, the dynamical behaviors of system (10) are similar to that of system (19). However, system (10) may not be able to replace system (19) in other regions. In regions D_{01} and D_{02}, system (10) may underestimate the outbreak of malaria. The reason is that for system (10), when $(\alpha, \delta) \in D_{01} \cup D_{02}$, malaria can be eliminated. As for system (19), bistability arises if $(\alpha, \delta) \in D_{01}$. Accordingly, the outbreak or eradication of malaria and the level of initial infection is vitally interrelated. When $(\alpha, \delta) \in D_{02}$, the endemic equilibrium E_2 of system (19) is the unique stable equilibrium, which implies outbreak of malaria. It is worth noting that for $(\alpha, \delta) \in D_{10}$, system (10) may overestimate the outbreak of disease. That is caused by the fact that system (10) possesses two endemic equilibria. Moreover, due to the occurrence of Bogdanov–Takens bifurcation, when the parameters change from region D_{11-1} to region D_{11-2}, the endemic equilibrium E_2 changes from unstable to stable; for $(\alpha, \delta) \in D_{11-2}$, the unstable periodic solution appears and surrounds E_2, and it ruptures through homoclinic loop. Hence system (10) may generate misjudgment. Figure 7 indicates that parameter area determines whether the dynamics of system (19) can be revealed by the dynamics of system (10).

5.4 Bifurcation diagram and dynamical behaviors for system (5)

According to the results in Sect. 4.3, system (5) can exhibit Turing–Hopf bifurcation at E_2. In this part, setting $\Omega = (0, 3.5\pi)$, α and r are selected as bifurcation parameters to depict bifurcation diagram.

Take

$$\begin{aligned} &N_h = 110,\ N_v = 220,\ b = 0.4,\ \beta_h = 0.07,\ \beta_v = 0.4,\ \theta = 0.018,\\ &\delta = 0.232,\ v = 0.00065,\ d_h = \frac{1}{70 \times 365},\ d_v = \frac{1}{25},\ d_1 = \frac{0.4}{30},\ d_2 = \frac{0.02}{30}, \end{aligned} \tag{30}$$

Table 5 Substitution results under different parameter regions

Parameter region	D_{00}	D_{01}	D_{02}
Substitution result	Yes	No	No
		(may underestimate)	(may underestimate)
Parameter region	D_{10}	D_{11-1}	D_{11-2}
Substitution result	No	No	No
	(may overestimate)	(may misjudge)	(may misjudge)
Parameter region	D_{11-3}	D_{12}	D_{22}
Substitution result	Yes	No	Yes
		(may underestimate)	

which are adjusted on the basis of Bai et al. (2018), Bousema et al. (2010), Wang et al. (2017), Chitnis et al. (2008).

Four critical curves in (α, r) plane are shown in Fig. 8a. It is easy to obtain L^* : $r = r_1$ by solving $\mathcal{R}_0 = 1$. Clearly, $\frac{\partial \mathcal{R}_0}{\partial r} = \frac{b^2 N_v \beta_h \beta_v}{N_h d_v (r+d_h+\delta)^2}(\frac{\theta(d_h+\delta)}{v+d_h} - 1)$. For these given parameters, $\frac{\partial \mathcal{R}_0}{\partial r} > 0$. Then $\mathcal{R}_0 < 1$ if $r < r_1$ and $\mathcal{R}_0 > 1$ if $r > r_1$. Note that $\alpha > \alpha_0$ holds when $r < r_1$. The curve L_0 is defined by solving $\mathcal{R}_0 = \mathcal{R}_0^+$. Further, introduce

$$\Omega_0 = \{(\alpha, r)|\ \mathcal{R}_0 < \mathcal{R}_0^+\},\ \Omega_1 = \{(\alpha, r)|\ \mathcal{R}_0^+ < \mathcal{R}_0 < 1\},\ \Omega_2 = \{(\alpha, r)|\ \mathcal{R}_0 > 1\}. \tag{31}$$

Hence based on Theorem 8, system (5) admits zero, two and one endemic equilibria in regions Ω_0, Ω_1 and Ω_2, respectively. Moreover, it follows from (B2) that $i^* = 1$. Besides, the black curve and blue curve represent Turing bifurcation and Hopf bifurcation, respectively. These two curves intersect at the point $TH = (\alpha^*, r^*) \approx (0.07504, 0.00144)$ satisfying the conditions in Theorem 18. Thereupon, for $\mathcal{R}_0 < 1$, system (5) admits (1,0)-mode Turing–Hopf bifurcation at $E_2 \approx (2.9382, 6.1467, 21.9562)^{\mathrm{T}}$ when $(\alpha, r) = (\alpha^*, r^*)$.

Moreover, normal form (G6) for (1,0)-mode Turing–Hopf bifurcation is given by

$$\begin{cases} \dfrac{\mathrm{d}z_1}{\mathrm{d}t} = 0.0005iz_1 + ((0.0129 - 0.1004i)\epsilon_1 + (-0.1392 + 0.64i)\epsilon_2)z_1 \\ \qquad\qquad + (-1.293 \times 10^{-7} - 1.2152 \times 10^{-7}i)z_1^2 z_2 \\ \qquad\qquad + (3.5435 \times 10^{-7} - 1.4481 \times 10^{-7}i)z_1 z_3^2, \\ \dfrac{\mathrm{d}z_2}{\mathrm{d}t} = -0.0005iz_2 + ((0.0129 + 0.1004i)\epsilon_1 + (-0.1392 - 0.64i)\epsilon_2)z_2 \\ \qquad\qquad + (-1.293 \times 10^{-7} + 1.2152 \times 10^{-7}i)z_1 z_2^2 \\ \qquad\qquad + (3.5435 \times 10^{-7} + 1.4481 \times 10^{-7}i)z_2 z_3^2, \\ \dfrac{\mathrm{d}z_3}{\mathrm{d}t} = (0.0386\epsilon_1 - 0.6832\epsilon_2)z_3 - 5.704 \times 10^{-7} z_1 z_2 z_3 - 7.0563 \times 10^{-8} z_3^3. \end{cases} \tag{32}$$

To discuss the dynamics, consider the transformations $z_1 = R\cos\Theta + iR\sin\Theta$, $z_2 = R\cos\Theta - iR\sin\Theta$, $z_3 = P$, and rescale $\rho_1 = \sqrt{1.293\times10^{-7}}R$, $\rho_2 = \sqrt{7.0563\times10^{-8}}P$. Dropping the differential equation of Θ, (32) is transformed into

$$\begin{cases} \dfrac{\mathrm{d}\rho_1}{\mathrm{d}t} = (0.0129\epsilon_1 - 0.1392\epsilon_2)\rho_1 - \rho_1^3 + 5.0218\rho_1\rho_2^2, \\ \dfrac{\mathrm{d}\rho_2}{\mathrm{d}t} = (0.0386\epsilon_1 - 0.6832\epsilon_2)\rho_2 - 4.4115\rho_1^2\rho_2 - \rho_2^3. \end{cases} \tag{33}$$

Notably, $\rho_1 \geq 0$ and ρ_2 is arbitrarily real number. Then system (33) admits equilibria

$$\begin{aligned} &J_0 = (0,0)^{\mathrm{T}}, \text{ for all } \epsilon_1,\ \epsilon_2, \\ &J_1 = \left(\sqrt{0.0129\epsilon_1 - 0.1392\epsilon_2}, 0\right)^{\mathrm{T}}, \text{ for } \epsilon_2 < 0.0927\epsilon_1, \\ &J_2^{\pm} = \left(0, \pm\sqrt{0.0386\epsilon_1 - 0.6832\epsilon_2}\right)^{\mathrm{T}}, \text{ for } \epsilon_2 < 0.0565\epsilon_1, \\ &J_3^{\pm} = \frac{1}{\sqrt{23.1536}}\left(\sqrt{-0.0184\epsilon_1 - 0.0692\epsilon_2}, \pm\sqrt{0.2067\epsilon_1 - 3.5698\epsilon_2}\right)^{\mathrm{T}}, \\ &\text{for } \epsilon_2 < -0.266\epsilon_1,\ \epsilon_2 < 0.0579\epsilon_1. \end{aligned}$$

Consequently, acquire critical bifurcation curves

$$\begin{aligned} &F_0 : \epsilon_2 = 0.0927\epsilon_1,\ T_1 : \epsilon_2 = 0.0565\epsilon_1, \\ &K_1 : \epsilon_2 = -0.266\epsilon_1,\ K_2 : \epsilon_2 = 0.0579\epsilon_1. \end{aligned}$$

Based on Guckenheimer and Holmes (1983), the unfolding for (33) is Case III. These critical lines F_0, T_1, K_1 and K_2 divide $\epsilon_1 - \epsilon_2$ plane into six regions shown in Fig. 8b. In each region, we list the existence and stability of these six equilibria for system (33), as shown in Table 6. Inspired by Song et al. (2016), the corresponding relationship between the equilibrium of system (33) and the equilibrium of system (5) is obtained. That is, J_0 represents the endemic equilibrium E_2 of system (5), and J_1 corresponds to spatially homogeneous periodic solution. Moreover, $J_2^{\pm}$ stand for spatially inhomogeneous steady states and $J_3^{\pm}$ match with spatially inhomogeneous periodic solutions. In view of Theorem 14, E_0 is locally asymptotically stable when $\mathcal{R}_0 < 1$. As a result, system (5) may exhibit bistability or tristability for $\mathcal{R}_0 < 1$. That is, the stable disease-free equilibrium may coexist with a stable endemic equilibrium E_2, or a stable spatial homogeneous periodic solution, or a pair of stable spatial inhomogeneous periodic solutions, or a pair of stable spatial inhomogeneous steady states. Biologically, malaria may show a variety of epidemic trends, such as elimination or inhomogeneous distribution in space and periodic fluctuation in time of infectious populations. Figures 14, 15 and 16 show multi-stability of system (5) in regions II, IV and VI, respectively.

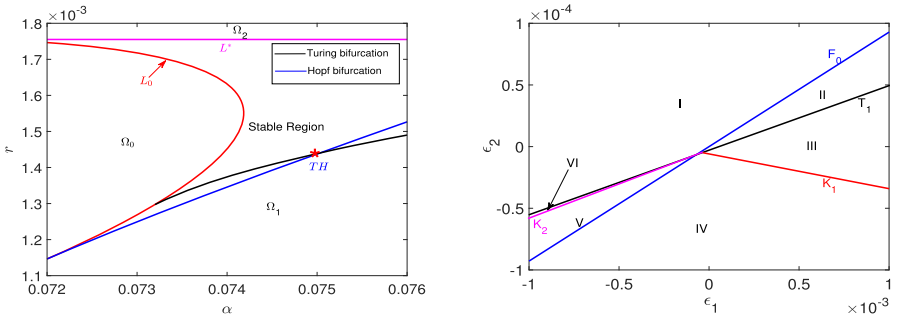

Fig. 8 Bifurcation curves of system (5) in **a** (α, r) plane, and **b** (ϵ_1, ϵ_2) plane

Table 6 The existence and stability of equilibria for system (33)

Region\Equilibria	J_0	J_1	$J_2^{\pm}$	$J_3^{\pm}$
I	Stable	Noexistence	Noexistence	Noexistence
II	Unstable	Stable	Noexistence	Noexistence
III	Unstable	Stable	Unstable	Noexistence
IV	Unstable	Unstable	Unstable	Stable
V	Unstable	Noexistence	Unstable	Stable
VI	Unstable	Noexistence	stable	Noexistence

5.5 The comparison between systems (5) and (6)

The previous analysis indicates that when (α, r) belongs to different regions, system (5) exhibits significantly different dynamic behaviors. While for two-compartment model (6), when the parameter takes value of (30), one arrives $(\alpha, r) \in \bar{\Omega}_1 = \{(\alpha, r) | \ \alpha > \tilde{\alpha}_0, \ \bar{\mathcal{R}}_0^+ < \bar{\mathcal{R}}_0 < 1\}$. This infers that system (6) always admits two endemic equilibria $\bar{E}_1$ and $\bar{E}_2$, which coexist with the DFE $\bar{E}_0$.

In order to further compare systems (5) and (6), introduce

$$N_1 = \bar{\Omega}_1 \cap \Omega_2, \ N_2 = \bar{\Omega}_1 \cap \Omega_0, \ N_3 = \bar{\Omega}_1 \cap \Omega_{1-1}, \ N_4 = \bar{\Omega}_1 \cap \Omega_{1-2},$$

in which Ω_{1-1} and Ω_{1-2} represent stable and unstable regions of the endemic equilibrium E_2, respectively. Accordingly, four subregions in (α, r) plane are shown in Fig. 9. If $(\alpha, r) \in N_3$, then the dynamics of system (6) are similar to that of system (5). While when (α, r) belongs to other regions, the dynamic behaviors of system (6) are significantly different from that of system (5). More specifically, for $(\alpha, r) \in N_1$, system (6) may underestimate the emergence of malaria. When $(\alpha, r) \in N_2$, system (6) may overestimate the outbreak of disease. Besides, if $(\alpha, r) \in N_4$, system (6) may misjudge the epidemic pattern of malaria. Thereby, parameter region has profound influence on whether the dynamics of system (6) can replace that of system (5).

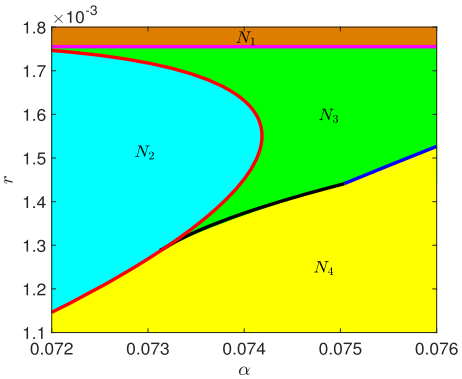

Fig. 9 The subregions of (α, r) plane

6 A numerical application to Burundi

Burundi, located in sub-Saharan Africa, is a country ravaged by malaria. This section is devoted to exploring the spread and control of malaria in Burundi. Firstly, based on surveillance data from Burundi (Burundi Ministry of Public Health and the Fight Against AIDS 2023), we estimate unknown parameter vector and calculate the basic reproduction number $\mathcal{R}_M$. Subsequently, sensitivity analysis is carried out to reveal the key parameters affecting malaria epidemic. At last, we assess the impact of parameters on malaria spread.

6.1 Data fitting

Use system (5) to fit cumulative malaria data. In the following, take $\Omega = (0, 1)$. The values of some parameters are shown in Table 7, however we are unable to obtain the values of remaining parameters since the lack of detailed information about malaria spread in Burundi. Motivated by Wang and Zhao (2022), Burundi Ministry of Public Health and the Fight Against AIDS (2023), take $N_v = gN_h$, $I_h(0) = c_1 N_h(-156.2x^5 + 390.6x^4 - 333.3x^3 + 115.6x^2 - 17.7x + 4)$, $R_h(0) = rI_h(0)$ and $I_v(0) = c_2 I_h(0)$. Hence, g, c_1, c_2 are treated as parameters for estimation.

Inspired by Shi et al. (2021), we design an algorithm based on BP neural network to estimate parameter vector $\Theta = (\alpha, g, c_1, c_2)$. Table 7 lists the estimation results. Under the baseline parameter values, Fig. 10 shows that system (5) matches the data reported by Burundi well. We calculate the basic reproduction number $\mathcal{R}_M \approx 1.71$. Theorem 15 infers that the endemic equilibrium $E_2 \approx (1288277, 7513551, 6933902)^{\mathrm{T}}$ is stable. It verifies that malaria is prevalent in Burundi.

6.2 Sensitivity analysis to $\mathcal{R}_0$ and $\mathcal{R}_0^+$

Theorem 8 illustrates that $\mathcal{R}_0$ and $\mathcal{R}_0^+$ play important role in the existence of equilibria. Now we identify key parameters that have significant impact on $\mathcal{R}_0$ and $\mathcal{R}_0^+$ by applying partial rank correlation coefficient (PRCC) method. As shown in Fig. 11a, the biting rate b and the total density of mosquitoes N_v are highly positively correlated with $\mathcal{R}_0$, while the cure recovery rate δ and the natural death rate of mosquito pop-

Table 7 Parameter values

Parameter	Value	References
N_h	1.25×10^7	(Wang and Zhao 2022)
d_v	0.026	(Chitnis et al. 2008)
b	0.28	(Chitnis et al. 2008)
β_v	0.48	(Chitnis et al. 2008)
β_h	0.02	(Chitnis et al. 2008)
d_h	$\frac{1}{63.5*365}$	(Wang and Zhao 2022)
r	0.009	(Wang and Zhao 2022; Chitnis et al. 2008)
v	0.0015	(Wang and Zhao 2022; Chitnis et al. 2008)
δ	0.01	(Wang and Zhao 2022; Feng et al. 2004)
θ	0.1	(Wang and Zhao 2022; Chitnis et al. 2008)
d_1	$\frac{0.4}{30}$	(Bai et al. 2018)
d_2	$\frac{0.02}{30}$	(Bai et al. 2018)
α	0.00001	Estimation
g	1.2	Estimation
c_1	0.018	Estimation
c_2	1.001	Estimation

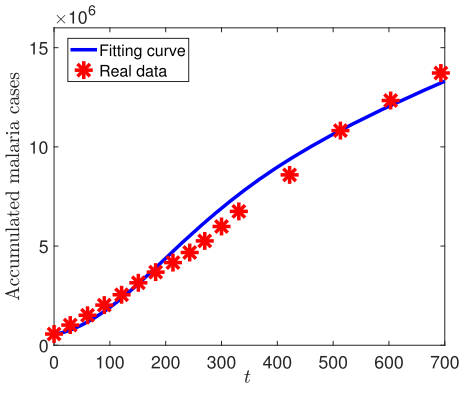

Fig. 10 The fitting results of real data in Burundi from 31 January 2021 to 31 December 2022

ulation d_v are highly negatively correlated with $\mathcal{R}_0$. $\mathcal{R}_0$ is moderate or insensitive to the change of remaining parameters. In addition, the natural recovery rate r is highly positively correlated with $\mathcal{R}_0^+$. The cure recovery rate δ and the extent of the delayed effect for treatment α are highly negatively correlated with $\mathcal{R}_0^+$. Other parameters have little effect on $\mathcal{R}_0^+$ (see Fig. 11b).

6.3 The contour plots of $\mathcal{R}_0$

In order to cope with the outbreak of malaria, humans can reduce the total density of mosquitoes N_v by spraying insecticides, reduce the biting rate b by strengthening

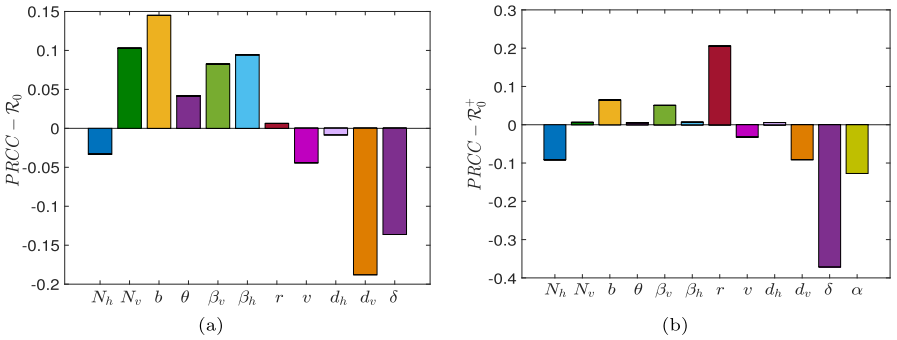

Fig. 11 Sensitivity analysis of **a** $\mathcal{R}_0$; **b** $\mathcal{R}_0^+$

personal protection, increase cure recovery rate δ by improving medical services and reduce the extent of the delayed effect for treatment α by increasing medical resources to cure patients in time. Besides, in view of $N_v = gN_h$, variation of N_v is reflected by variation of g. Next, illustrate the dependence of $\mathcal{R}_0$ on controllable parameters (i.e., g, b, δ and α).

Figure 12 shows the contour plots of $\mathcal{R}_0$ with respect to controllable parameters. Curves L_0 and L_1 stand for $\mathcal{R}_0 = \mathcal{R}_0^+$ and $\alpha = \alpha_0$, respectively. Further, define parameter regions

$$W_1 = \{(k_1, k_2) |\ \alpha > \alpha_0,\ \mathcal{R}_0 < \mathcal{R}_0^+\},\ W_2 = \{(k_1, k_2) |\ \alpha < \alpha_0,\ \mathcal{R}_0 < 1\},$$

where $(k_1, k_2) \in \{(g, b), (g, \delta), (b, \delta), (g, \alpha), (b, \alpha), (\delta, \alpha)\}$. Based on the previous analysis, when parameters belong to $W_0 = W_1 \cup W_2$, the DFE E_0 is unique equilibrium, which is locally asymptotically stable. Accordingly, it is beneficial to eliminate malaria by adjusting the parameters to within W_0. In detail, when g is kept at the current level, $(g, b) \in W_0$ if $b < 0.14$. If b is fixed at the current level, then $(g, b) \in W_0$ for $g < 0.33$. In addition, for any $b \in [0.1, 1]$, we have $\mathcal{R}_0 > 1$ as $g > 3.21$ (see Fig. 12a). Keeping g unchanged, $(g, \delta) \in W_0$ if $\delta > 0.13$ (see Fig. 12b). Figure 12c indicates that for any $\delta \in [0.001, 0.25]$, we obtain $\mathcal{R}_0 > 1$ as $b > 0.61$. Figure 12d–f illustrate that α does not affect $\mathcal{R}_0$. While, it can be used for disease control. Therefore, reducing the total density of mosquitoes, reducing the biting rate and reducing the delayed effect for treatment, as well as improving the treatment recovery rate have profound impact on malaria control.

6.4 The impact of controllable parameters on malaria spread

This part aims to assess the effect of controllable parameters on $\mathcal{R}_0$ and the number of cases under the same change percentage. Here change percentage refers to percentage of decrease for g, b and α, and percentage of increase for δ. Inspired by Abboubakar et al. (2018), introduce the efficiency index $\mathcal{B}$ to evaluate the influence of parameters

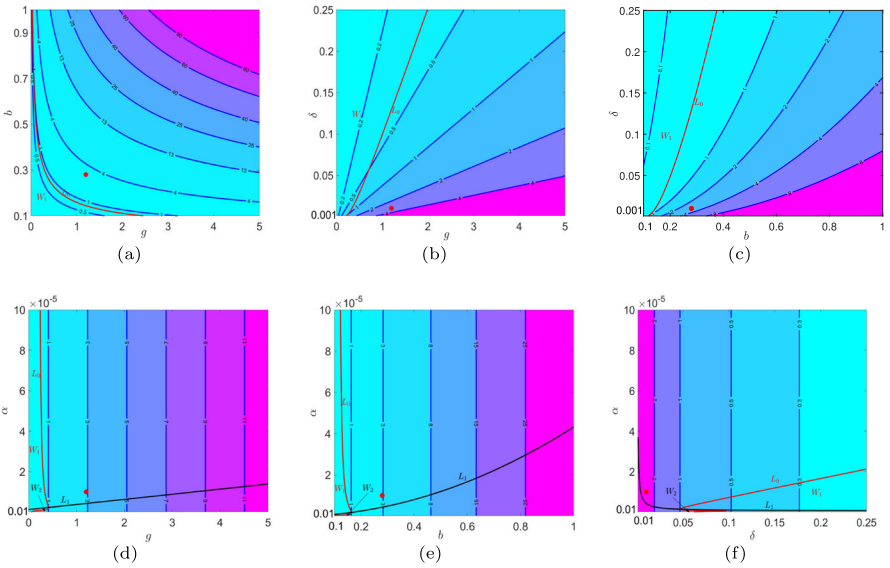

Fig. 12 The contour plots of $\mathcal{R}_0$ with respect to **a** g and b, **b** g and δ, **c** b and δ, **d** g and α, **e** b and α and **f** δ and α. Here red dot indicates the current level (color figure online)

on the number of cases. $\mathcal{B}$ is defined as follows

$$\mathcal{B} = \left(1 - \frac{A_h^c}{A_h^0}\right) \times 100\%,$$

where $A_h^0 = \int_0^T \int_\Omega I_h^0(t,x)\mathrm{d}x\mathrm{d}t$ and $A_h^c = \int_0^T \int_\Omega I_h^c(t,x)\mathrm{d}x\mathrm{d}t$, in which $T = 699$ represents the time interval from 31 January 2021 to 31 December 2022, $I_h^0(t,x)$ and $I_h^c(t,x)$ stand for infected persons under the baseline parameter values and that under adjusted parameter values, respectively. Further, in order to achieve the above objective, three scenarios are proposed:

Scenario 1 : only one controllable parameter is changed.

Scenario 2 : two controllable parameters are changed.

Scenario 3 : more than two controllable parameters are changed.

Figure 13 reveals the relationship between change percentage of parameters and $\mathcal{R}_0$ as well as $\mathcal{B}$ in each scenario. In scenario 1, when g is reduced by more than 73% or b is reduced by more than 49%, malaria can be eliminated (see Fig. 13a). Figure 13d implies that when parameters g, b, δ and α change by 95%, $\mathcal{B}$ is 95.7%, 96.4%, 3.6% and 30.4%, respectively. Besides, reducing the biting rate has the greatest influence on $\mathcal{B}$, followed by reducing the total density of mosquitoes, then reducing the delayed effect of treatment and finally improving the treatment rate. Accordingly, in scenario 1, reducing the biting rate is the most effective for malaria control.

In scenario 2, except for the combination of δ and α, the other combinations are beneficial to the elimination of malaria. Moreover, the combination with b has greater influence on $\mathcal{R}_0$ than the combination without b. Specifically, if g and b change by

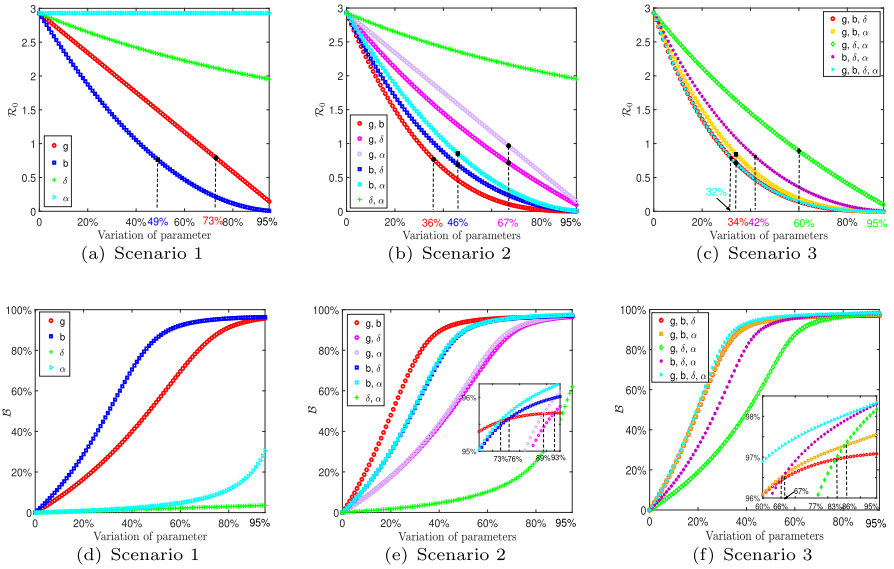

Fig. 13 The value of $\mathcal{R}_0$ under different change percentage of parameters among **a** scenario 1, **b** scenario 2 and **c** scenario 3. The efficiency index under different change percentage of parameters among **d** scenario 1, **e** scenario 2 and **f** scenario 3

more than 36% or g and δ change by more than 67%, malaria can be eliminated (see Fig. 13b). As shown in Fig. 13 (e), when the variation intensity is less than 73%, the influence on $\mathcal{B}$ is combination of g and b, b and α, b and δ, g and α, g and δ and δ and α in descending order. If the change of b and α is more than 73%, or that of b and δ is more than 76%, or that of g and α is more than 89%, or that of g and δ is more than 93%, then the corresponding value of $\mathcal{B}$ will exceed the value of $\mathcal{B}$ under the combination of g and b, nevertheless the difference between the values of $\mathcal{B}$ is less than 1%. From the perspective of reducing the number of cases, when the change percentage is less than 73%, the most effective way is to reduce the biting rate and the total density of mosquitoes; otherwise, the combination of reducing the biting rate and reducing the delayed effect for treatment is the most effective.

In scenario 3, each combination can eliminate malaria under suitable percentage of change. The combination of g, b, δ and α requires variation of more than 32%. For the combination of g, δ and α, the variation needs to exceed 60%. In addition, when three controllable parameters are adjusted, the combination of g, b and δ has greater influence on $\mathcal{R}_0$ than other three combinations (see Fig. 13c). Moreover, when the change percentage is less than 66%, this combination has the greatest influence on $\mathcal{B}$. When the change percentage is higher than 66%, the value of $\mathcal{B}$ under this combination may be lower than that of $\mathcal{B}$ under the other three combinations, but the difference between $\mathcal{B}$ values not exceed 1.5%. Notably, in scenario 3, combining all available measures is the most effective way to reduce the number of cases. If only three controllable parameters are adjusted, when the change percentage is less than 66%, the most effective combination is to reduce the biting rate, the total density of mosquitoes

and the delayed effect for treatment; otherwise, the combination of improving the treatment recovery rate, reducing the biting rate and reducing the delayed effect for treatment is the most effective.

7 Discussion

In view of the slight infectivity of natural recovery persons, our interest is whether neglecting this factor in areas with limited medical resources can simplify analysis and retain significant dynamics. In order to answer this problem, introduce and analyze two-compartment and three-compartment models in both scenarios without and with spatial diffusion. This enables us to find key parameters that possess important influence on malaria epidemic trends, thus providing insights for transmission and control of malaria.

In the absence of spatial movement, there are significant differences between the dynamics of two-compartment model (10) and three-compartment model (19). More specifically, model (10) can undergo backward bifurcation. However, model (19) can admit not only backward bifurcation, but also Hopf bifurcation and Bogdanov–Takens bifurcation. Further, parameter regions are given to illustrate whether the dynamics of model (19) can be revealed by that of model (10). When there is no endemic equilibrium in both models (10) and (19), model (10) can replace model (19). In this case, the infectivity of natural recovery individuals can be neglected. Otherwise, compared to model (19), model (10) may underestimate, overestimate or misjudge the prevalence of malaria. Under the case, the infectivity of natural recovery persons may not be overlooked. It is necessary to set up suitable compartments for malaria model, since the epidemic mode of malaria cannot be presented by simpler analysis.

The analysis and dynamics of spatial two-compartment model (6) are relatively simple, while that of spatial three-compartment model (5) are complex and interesting. For model (5), with the help of Shengjin's Distinguishing Means, the stability analysis is better completed. In addition, it can admit Turing instability, Hopf bifurcation and Turing–Hopf bifurcation. Further, the normal form of Turing–Hopf bifurcation is given, in which the details are different from those of Turing–Hopf bifurcation for two-compartment model (Song et al. 2016). Numerically, when the basic reproduction number $\mathcal{R}_M$ is less than one, model (5) may allow the appearance of bistable or even tristable phenomena. Here, bistable and tristable patterns imply that the stable disease-free equilibrium may coexist with a stable endemic equilibrium, or a stable spatial homogeneous periodic solution or a pair of stable spatial inhomogeneous periodic solutions, or a pair of stable spatial inhomogeneous steady states, respectively. Biologically, for $\mathcal{R}_M < 1$, there may be various epidemic trends of malaria, such as elimination or inhomogeneous distribution in space and cyclic fluctuation in time of infectious classes. In the previous research on reaction-diffusion epidemic model (Sun 2012; Wang et al. 2018; Zhu and He 2022), under the same parameters, the model can exhibit bistability, but rarely show tristability. Accordingly, the tristable phenomenon in our model seems to be a new discovery.

Notice that the replacement results of spatial two-compartment model for spatial three-compartment model are similar to that of their corresponding non-spatial

versions. The difference is that in the presence of spatial diffusion, spatial two-compartment model (6) may bring misjudgment due to Turing instability, Hopf bifurcation and Turing–Hopf bifurcation for spatial three-compartment model (5). While in the absence of spatial diffusion, non-spatial two-compartment model (10) may cause misjudgment due to Hopf bifurcation and Bogdanov–Takens bifurcation for non-spatial three-compartment (19). Compared with Wang and Zhao (2022), Lou and Zhao (2010), our results provide new perspective for understanding the role of the infectivity of natural recovery category in malaria spread in both scenarios without and with spatial diffusion.

In addition, the delayed effect for treatment does not affect the basic reproduction number of the model, but may affect the existence and stability of equilibria. To be specific, if there is no delayed effect for treatment in non-spatial two-compartment and three-compartment models, then these two models do not experience any other bifurcations except for the forward bifurcation. When the delayed effect for treatment is not considered in spatial two-compartment and three-compartment models, the dynamics of these two models are relatively simple, without Turing instability, Hopf bifurcation and Turing–Hopf bifurcation. These results mean that ignoring the delayed effect for treatment may underestimate the emergence of malaria and misjudge the epidemic pattern at the time of disease outbreak. Therefore, the delayed effect for treatment plays significant role in malaria transmission.

At last, spatial three-compartment model is applied to exhibit the transmission of malaria in Burundi. Based on the cumulative malaria data reported in Burundi, the unknown parameters are estimated, thus acquiring $\mathcal{R}_M \approx 1.71$. This demonstrates that malaria is prevalent in Burundi. The critical thresholds (i.e., $\mathcal{R}_0$ and $\mathcal{R}_0^+$) are used to determine the preferred strategy for eliminating malaria. The efficiency index is applied to identify the preferred method for reducing malaria cases. Specifically, it is the most effective to simultaneously take all available measures to improve the treatment recovery rate and reduce the total density of mosquitoes, the biting rate and the delayed effect for treatment. If only three types of measures are taken, when the change percentage is less than 66%, the most effective combination is to reduce the biting rate, the total density of mosquitoes and the delayed effect for treatment; otherwise, the combination of improving the treatment recovery rate, reducing the biting rate and reducing the delayed effect for treatment is the most effective. When only two types of measures are implemented, if the change percentage is less than 73%, then the most effective way is to reduce the biting rate and the total density of mosquitoes; otherwise, the combination of reducing the biting rate and reducing the delayed effect for treatment is the most effective. If only one type of measure is taken, then reducing the biting rate is the most effective. We hope that these conclusions can provide theoretical basis for malaria control in Burundi.

Acknowledgements The authors are grateful to the editor and the anonymous reviewers for their careful reading and valuable suggestions, which have led to substantial improvements in the manuscript. The first two authors are partially supported by the National Natural Science Foundation of China (Nos. 11971013, 12371490). The third author is partially supported by the Natural Sciences and Engineering Research Council of Canada (Individual Discovery Grant RGPIN-2020-03911 and Discovery Accelerator Supplement Award RGPAS-2020-00090).

Declarations

Conflict of interest The authors declare that they have no conflict of interest.

Appendix A: Proof of Theorem2

Proof Due to

$$\bar{Q}_0 > 0 \Leftrightarrow \bar{\mathcal{R}}_0 < 1; \quad \bar{Q}_0 = 0 \Leftrightarrow \bar{\mathcal{R}}_0 = 1; \quad \bar{Q}_0 < 0 \Leftrightarrow \bar{\mathcal{R}}_0 > 1,$$

$\bar{g}(I_h) = 0$ admits a unique positive solution for $\bar{Q}_0 < 0$. Thereby, as $\bar{\mathcal{R}}_0 > 1$, system admits a unique endemic equilibrium $\bar{E}_2$.

If $\bar{\mathcal{R}}_0 < 1$, then (9) has two positive roots when $\bar{Q}_1 < 0$ and $\Delta > 0$, and (9) has no positive roots when $\bar{Q}_1 \geq 0$. Moreover, $\bar{Q}_1 < 0$ if and only if $\bar{\mathcal{R}}_0 > \bar{P}_0$. Clearly, if $\bar{P}_0 \geq 1$, then system has no endemic equilibrium when $\bar{\mathcal{R}}_0 < 1$. In addition, one yields that

$$\bar{P}_0 < 1 \Leftrightarrow \alpha > \bar{\alpha}_0, \ \Delta > 0 \Leftrightarrow 0 < \bar{\mathcal{R}}_0 < \max\{0, \ \bar{\mathcal{R}}_0^-\} \text{ or } \bar{\mathcal{R}}_0 > \bar{\mathcal{R}}_0^+.$$

Thus, for $\alpha > \bar{\alpha}_0$ and $\bar{\mathcal{R}}_0^+ < \bar{\mathcal{R}}_0 < 1$, there are two endemic equilibria $\bar{E}_1$ and $\bar{E}_2$.

For $\bar{\mathcal{R}}_0 = 1$ and $\alpha > \bar{\alpha}_0$, $\bar{Q}_0 = 0$ and $\bar{Q}_1 < 0$. Hence, system admits a unique endemic equilibrium $\bar{E}_2$.

When $\bar{\mathcal{R}}_0 = \bar{\mathcal{R}}_0^+$ and $\alpha > \bar{\alpha}_0$, we have $\Delta = 0$, $\bar{Q}_0 > 0$ and $\bar{Q}_1 < 0$. So, there is a unique endemic equilibrium $\bar{E}_1 = \bar{E}_2$.

When $\alpha > \bar{\alpha}_0$, $\Delta < 0$ if $\bar{P}_0 < \bar{\mathcal{R}}_0 < \bar{\mathcal{R}}_0^+$ and $\bar{Q}_1 \geq 0$ if $\bar{\mathcal{R}}_0 \leq \bar{P}_0$. Accordingly, for $\bar{\mathcal{R}}_0 < \bar{\mathcal{R}}_0^+$ and $\alpha > \bar{\alpha}_0$, system has no endemic equilibrium.

If $\bar{\mathcal{R}}_0 \leq 1$ and $\alpha \leq \bar{\alpha}_0$, then $\bar{Q}_1 \geq 0$ and $\bar{Q}_0 \geq 0$. Accordingly, there is no endemic equilibrium. Thereby, we complete the proof. □

Appendix B: Proof of Theorem 4:

Proof Direct calculation yields the local stability of equilibria. Below, we mainly prove the global stability of $\bar{E}_0$ and $\bar{E}_2$.

When $\bar{E}_0$ is a unique equilibrium of system (10), according to Poincaré-Bendixson Theorem, there is no periodic orbits in $\bar{\Gamma}$. The local stability of $\bar{E}_0$ implies that it is globally asymptotically stable (Brauer and Castillo-Chavez 2012). Thus, Theorem 4 (i) is valid.

Next, Bendixson's theorem is applied to illustrate the nonexistence of the limit cycle. Let

$$\check{P}_1(I_h, I_v) = b\beta_h \frac{I_v}{N_h}(N_h - I_h) - \frac{\delta I_h}{1 + \alpha I_h} - r I_h - d_h I_h,$$
$$\check{Q}_1(I_h, I_v) = b\beta_v \frac{I_h}{N_h}(N_v - I_v) - d_v I_v.$$

One can get

$$\frac{\partial \check{P}_1}{\partial I_h} + \frac{\partial \check{Q}_1}{\partial I_v} = -\frac{b\beta_h}{N_h} I_v - \frac{\delta}{(1+\alpha I_h)^2} - r - d_h - \frac{b\beta_v I_h}{N_h} - d_v < 0 \; in \; \bar{\Gamma}.$$

This implies that there is no limit cycle in $\bar{\Gamma}$. When $\bar{\mathcal{R}}_0 > 1$, $\bar{E}_2$ is a unique locally asymptotically stable equilibrium of system (10). Accordingly, it must be globally asymptotically stable in $\bar{\Gamma} \setminus \{\bar{E}_0\}$ (Brauer and Castillo-Chavez 2012). Thus, Theorem 4 (iii) is established. □

Appendix C: Proof of Theorem 5:

Proof System (10) can be written as

$$\frac{\mathrm{d}w}{\mathrm{d}t} = \bar{f}(w)$$

with $w = (w_1, w_2)^{\mathrm{T}} = (I_h, I_v)^{\mathrm{T}}$, and $\bar{f} = (\bar{f}_1, \bar{f}_2)^{\mathrm{T}}$ is shown below

$$\begin{cases} \bar{f}_1 = \bar{\beta}_h w_2 (N_h - w_1) - \dfrac{\delta w_1}{1+\alpha w_1} - r w_1 - d_h w_1, \\ \bar{f}_2 = \bar{\beta}_v w_1 (N_v - w_2) - d_v w_2. \end{cases}$$

Select δ as the bifurcation parameter. From $\bar{\mathcal{R}}_0 = 1$, we have $\delta = \bar{\delta}_1$. Let $\phi = \bar{\delta}_1 - \delta$. At $\phi = 0$, the Jacobian matrix of system (10) at the DFE $\bar{E}_0$, denoted by $J(\bar{E}_0)|_{\phi=0}$, admits a zero eigenvalue and an eigenvalue with negative real part.

The left and right eigenvectors of $J(\bar{E}_0)|_{\phi=0}$ related to zero eigenvalue are

$$p = (p_1, p_2) = \left(\frac{\bar{\beta}_v N_v}{r + d_h + \bar{\delta}_1}, 1 \right) p_2, \; q = (q_1, q_2)^{\mathrm{T}} = \left(\frac{d_v}{\bar{\beta}_h N_h}, 1 \right)^{\mathrm{T}} q_2,$$

respectively, where $q_2 > 0$ satisfying Theorem 4.1 in Castillo-Chavez and Song (2004). Furthermore, p_2 and q_2 can be selected to satisfy $p_2 q_2 = \frac{(r+d_h+\bar{\delta}_1)\bar{\beta}_h N_h}{\bar{\beta}_v N_v d_v + (r+d_h+\bar{\delta}_1)\bar{\beta}_h N_h} > 0$ such that $p \cdot q = 1$.

In addition,

$$\frac{\partial^2 \bar{f}_1}{\partial w_1^2}(0,0) = 2\alpha\bar{\delta}_1, \; \frac{\partial^2 \bar{f}_1}{\partial w_1 \partial w_2}(0,0) = \frac{\partial^2 \bar{f}_1}{\partial w_2 \partial w_1}(0,0) = -\bar{\beta}_h,$$
$$\frac{\partial^2 \bar{f}_2}{\partial w_1 \partial w_2}(0,0) = \frac{\partial^2 \bar{f}_2}{\partial w_2 \partial w_1}(0,0) = -\bar{\beta}_v, \; \frac{\partial^2 \bar{f}_1}{\partial w_1 \partial \phi}(0,0) = 1,$$

and remaining derivatives are equal to zero.

Based on Theorem 4.1 in Castillo-Chavez and Song (2004), the coefficients $\tilde{a}$ and $\tilde{b}$ are

$$\tilde{a} = \sum_{k,i,j=1}^{2} p_k q_i q_j \frac{\partial^2 \bar{f}_k}{\partial w_i \partial w_j}(0,0) = \frac{2\bar{\beta}_h \bar{\delta}_1 N_h d_v}{(r + d_h + \bar{\delta}_1)^2} p_2 q_2^2 (\alpha - \bar{\alpha}_1),$$

$$\tilde{b} = \sum_{k,i=1}^{2} \bar{p}_k \bar{q}_i \frac{\partial^2 \bar{f}_k}{\partial w_i \partial \phi}(0,0) = \frac{\bar{\beta}_h \bar{\beta}_v N_h N_v}{(r + d_h + \bar{\delta}_1)^2} p_2 q_2 > 0.$$

Accordingly, system (10) undergoes, at $\bar{\mathcal{R}}_0 = 1$, a backward bifurcation as $\alpha > \bar{\alpha}_1$, and a forward bifurcation as $\alpha < \bar{\alpha}_1$. □

Appendix D: Proof of Theorem 10:

Direct calculation can obtain the local stability of equilibria. Next, applying geometric singular perturbation theory (Feng et al. 2004; Fenichel 1979), introduce the reduced system corresponding to system (19)

$$\begin{cases} \dfrac{\mathrm{d}I_h}{\mathrm{d}s} = \bar{\beta}_h \dfrac{\bar{\beta}_v (I_h + \theta R_h) N_v}{\bar{\beta}_v (I_h + \theta R_h) + d_v} (N_h - I_h - R_h) - \bar{r} I_h - \dfrac{\bar{\delta} I_h}{1 + \alpha I_h} - \bar{d}_h I_h, \\ \dfrac{\mathrm{d}R_h}{\mathrm{d}s} = \bar{r} I_h - \bar{v} R_h - \bar{d}_h R_h, \end{cases} \tag{D1}$$

where $\varepsilon = \frac{d_h}{d_v}, s = \varepsilon t, d_h = \varepsilon \bar{d}_h, \frac{b\beta_h}{N_h} = \varepsilon \bar{\beta}_h, \delta = \varepsilon \bar{\delta}, v = \varepsilon \bar{v}, r = \varepsilon \bar{r}, \bar{\beta}_v = \frac{b\beta_v}{N_h}$. Due to the facts that systems (19) and (D1) in this work correspond to systems (58) and (27) in Wang and Zhao (2022), and Wang and Zhao (2022) provides detailed derivation of the dynamics for reduced system (27) that can reveal the dynamics of system (58), we directly apply these results. Specifically, the stability of $\hat{E}_0 = (0,0)^{\mathrm{T}}$ in system (D1) is consistent with that of E_0 in system (19). Hence, the global stability of the DFE E_0 in system (19) is demonstrated by studying the global stability of the DFE $\hat{E}_0$ in reduced system (D1).

For system (D1), $\hat{\Gamma} = \{(I_h, R_h)^{\mathrm{T}} | 0 \le I_h \le N_h,\ 0 \le R_h \le N_h\}$ is positively invariant. If E_0 is a unique equilibrium of system (19), then $\hat{E}_0$ is a unique equilibrium of system (D1) Wang and Zhao (2022). According to Poincaré-Bendixson Theorem, system (D1) admits no periodic orbits in $\hat{\Gamma}$. Since the local stability of E_0 means the local stability of $\hat{E}_0$, the local stability of $\hat{E}_0$ implies that it is globally asymptotically stable in $\hat{\Gamma}$ (Brauer and Castillo-Chavez 2012). Thus, Theorem 10 is valid.

Appendix E: Proof of Corollary 3:

After some calculations, we obtain the local stability of equilibria. For $\alpha = 0$, similar to the proof of Theorem 10, the global stability of E_0 and E_3 in system (19) is obtained

by proving the global stability of $\hat{E}_0$ and $\hat{E}_3 = (I_{h3}, R_{h3})^{\mathrm{T}}$ in reduced system (D1) (Wang and Zhao 2022).

When E_0 is a unique equilibrium of system (19), $\hat{E}_0$ is a unique equilibrium of system (D1). Similar to the proof of Theorem 4 (i) and Theorem 10 (i), its local stability means its global stability. Thus, Corollary 3 (i) is valid.

In the following, Dulac's criterion is applied to prove the nonexistence of the limit cycle. Let

$$\check{P}_2(I_h, R_h) = \bar{\beta}_h \frac{\bar{\beta}_v(I_h + \theta R_h)N_v}{\bar{\beta}_v(I_h + \theta R_h) + d_v}(N_h - I_h - R_h) - \bar{r} I_h - \bar{\delta} I_h - \bar{d}_h I_h,$$
$$\check{Q}_2(I_h, R_h) = \bar{r} I_h - \bar{v} R_h - \bar{d}_h R_h,$$

and take Dulac function $\check{D} = \frac{\bar{\beta}_v(I_h+\theta R_h)+d_v}{I_h+\theta R_h}$. We have

$$\frac{\partial(\check{D}\check{P}_2)}{\partial I_h} + \frac{\partial(\check{D}\check{Q}_2)}{\partial I_v} = -\bar{\beta}_h\bar{\beta}_v N_v - \bar{\beta}_v(\bar{\delta} + \bar{r} + \bar{d}_h) - d_v(\bar{\delta} + \bar{r} + \bar{d}_h)\frac{\theta R_h}{(I_h + \theta R_h)^2}$$
$$- d_v(\bar{r}\theta + \bar{v} + \bar{d}_h)\frac{I_h}{(I_h + \theta R_h)^2} - \bar{\beta}_v(\bar{v} + \bar{d}_h) < 0 \; in \; \hat{\Gamma}\backslash\{\hat{E}_0\}.$$

This implies that there is no limit cycle in $\hat{\Gamma}\backslash\{\hat{E}_0\}$. When $\mathcal{R}_0 > 1$, E_3 is a unique locally asymptotically stable equilibrium of system (19) with $\alpha = 0$. Then $\hat{E}_3$ is a unique locally asymptotically stable equilibrium of system (D1) with $\alpha = 0$. Hence, $\hat{E}_3$ must be globally asymptotically stable in $\hat{\Gamma}\backslash\{\hat{E}_0\}$ (Brauer and Castillo-Chavez 2012). Therefore, Corollary 3 (ii) holds.

Appendix F: The definitions of b_{20}, c_{20} and c_{11}

$$a_1^1 = -\bar{\beta}_h I_v^* - d_h - r - \frac{\delta}{(1+\alpha I_h^*)^2},\ a_2^1 = -\bar{\beta}_h I_v^*,\ a_3^1 = \bar{\beta}_h(N_h - I_h^* - R_h^*),\ a_1^2 = r,$$
$$a_2^2 = -(v + d_h),\ a_1^3 = \bar{\beta}_v(N_v - I_v^*),\ a_2^3 = \theta\bar{\beta}_v(N_v - I_v^*),\ a_3^3 = -\bar{\beta}_v(I_h^* + \theta R_h^*) - d_v,$$
$$a_{11}^1 = \frac{\delta\alpha}{(1+\alpha I_h^*)^3},\ a_{13}^1 = -\bar{\beta}_h,\ a_{23}^1 = -\bar{\beta}_h,\ a_{13}^3 = -\bar{\beta}_v,\ a_{23}^3 = -\theta\bar{\beta}_v,$$
$$v_{11} = a_2^2 a_3^3,\ v_{21} = -a_1^2 a_3^3,\ v_{31} = -a_1^3 a_2^2 + a_2^3 a_1^2,\ v_{12} = -a_3^3,\ v_{22} = 0,\ v_{32} = \frac{a_3^3(a_2^2 + a_1^1)}{a_3^1},$$

$$v_{13} = (a_1^1 + a_3^3)(a_1^1 + a_2^2),\ v_{23} = a_1^2(a_1^1 + a_2^2),\ v_{33} = a_1^3(a_1^1 + a_3^3) + a_2^3 a_1^2,$$
$$T_{11} = -\frac{v_{32}v_{23}}{|T|},\ T_{21} = \frac{v_{31}v_{23} - v_{21}v_{33}}{|T|},\ T_{13} = \frac{v_{12}v_{23}}{|T|},\ T_{23} = \frac{v_{21}v_{13} - v_{11}v_{23}}{|T|},$$
$$b_{20} = T_{11}(a_{11}^1 v_{11}^2 + a_{13}^1 v_{11}v_{31} + a_{23}^1 v_{21}v_{31}) + T_{13}(a_{13}^3 v_{11}v_{31} + a_{23}^3 v_{21}v_{31}),$$
$$c_{20} = T_{21}(a_{11}^1 v_{11}^2 + a_{13}^1 v_{11}v_{31} + a_{23}^1 v_{21}v_{31}) + T_{23}(a_{13}^3 v_{11}v_{31} + a_{23}^3 v_{21}v_{31}),$$
$$c_{11} = T_{21}(2a_{11}^1 v_{11}v_{12} + a_{13}^1(v_{12}v_{31} + v_{11}v_{32}) + a_{23}^1(v_{31}v_{22} + v_{21}v_{32}))$$
$$+ T_{23}(a_{13}^3(v_{12}v_{31} + v_{11}v_{32}) + a_{23}^3(v_{31}v_{22} + v_{21}v_{32}))$$

with $|T| = v_{12}(v_{31}v_{23} - v_{21}v_{33}) + v_{32}(v_{21}v_{13} - v_{11}v_{23})$.

Appendix G: The normal form of Turing–Hopf bifurcation at E_2

Using the method in Song et al. (2016), we derive the normal form of Turing–Hopf bifurcation at E_2. We first introduce perturbation vector $\epsilon = (\epsilon_1, \epsilon_2)$ and make $\alpha = \alpha^* + \epsilon_1$ and $r = r^* + \epsilon_2$. Then system (5) reads as

$$\begin{cases} \dfrac{\partial I_h}{\partial t} = d_1\Delta I_h + \bar{\beta}_h I_v(N_h - I_h - R_h) - \dfrac{\delta I_h}{1 + (\alpha^* + \epsilon_1)I_h} \\ \qquad - (r^* + \epsilon_2)I_h - d_h I_h, & t > 0,\ x \in \Omega, \\ \dfrac{\partial R_h}{\partial t} = d_1\Delta R_h + (r^* + \epsilon_2)I_h - d_h R_h - vR_h, & t > 0,\ x \in \Omega, \\ \dfrac{\partial I_v}{\partial t} = d_2\Delta I_v + \bar{\beta}_v(I_h + \theta R_h)(N_v - I_v), & t > 0,\ x \in \Omega, \\ \dfrac{\partial I_h}{\partial n} = \dfrac{\partial R_h}{\partial n} = \dfrac{\partial I_v}{\partial n} = 0, & x \in \partial\Omega. \end{cases} \tag{G2}$$

Note that E_2 is still the endemic equilibrium of system (G2).

Taking the transformation $\xi_1 = I_h - I_{h2}$, $\xi_2 = R_h - R_{h2}$, $\xi_3 = I_v - I_{v2}$, one has

$$\begin{cases} \dfrac{\partial \xi_1}{\partial t} = d_1\Delta\xi_1 + f_1(\xi_1 + I_{h2}, \xi_2 + R_{h2}, \xi_3 + I_{v2}), & t > 0,\ x \in \Omega, \\ \dfrac{\partial \xi_2}{\partial t} = d_1\Delta\xi_2 + f_2(\xi_1 + I_{h2}, \xi_2 + R_{h2}, \xi_3 + I_{v2}), & t > 0,\ x \in \Omega, \\ \dfrac{\partial \xi_3}{\partial t} = d_2\Delta\xi_3 + f_3(\xi_1 + I_{h2}, \xi_2 + R_{h2}, \xi_3 + I_{v2}), & t > 0,\ x \in \Omega, \\ \dfrac{\partial \xi_1}{\partial n} = \dfrac{\partial \xi_2}{\partial n} = \dfrac{\partial \xi_3}{\partial n} = 0, & t > 0,\ x \in \partial\Omega, \end{cases} \tag{G3}$$

with

$$\begin{aligned} f_1(\xi_1 + I_{h2}, \xi_2 + R_{h2}, \xi_3 + I_{v2}) &= \bar{\beta}_h(\xi_3 + I_{v2})(N_h - \xi_1 - I_{h2} - \xi_2 - R_{h2}) \\ &\quad - \frac{\delta(\xi_1 + I_{h2})}{1 + (\alpha^* + \epsilon_1)(\xi_1 + I_{h2})} \\ &\quad - (r^* + \epsilon_2)(\xi_1 + I_{h2}) - d_h(\xi_1 + I_{h2}), \\ f_2(\xi_1 + I_{h2}, \xi_2 + R_{h2}, \xi_3 + I_{v2}) &= (r^* + \epsilon_2)(\xi_1 + I_{h2}) - (d_h + v)(\xi_2 + R_{h2}), \\ f_3(\xi_1 + I_{h2}, \xi_2 + R_{h2}, \xi_3 + I_{v2}) &= \bar{\beta}_v\left(\xi_1 + I_{h2} + \theta(\xi_2 + R_{h2})\right)(N_v - \xi_3 - I_{v2}) \\ &\quad - d_v(\xi_3 + I_{v2}). \end{aligned}$$

Letting $U = (\xi_1, \xi_2, \xi_3)^{\mathrm{T}}$ and

$$L(\epsilon) = \begin{pmatrix} -\bar{\beta}_h I_{v2} - \frac{\delta}{(1+(\alpha^*+\epsilon_1)I_{h2})^2} - r^* - \epsilon_2 - d_h & -\bar{\beta}_h I_{v2} & \bar{\beta}_h m_5 \\ r^* + \epsilon_2 & -v - d_h & 0 \\ \bar{\beta}_v(N_v - I_{v2}) & \theta\bar{\beta}_v(N_v - I_{v2}) & -m_3 \end{pmatrix},$$

system (G3) takes the following form

$$\frac{\partial U}{\partial t} = \mathcal{L}U + \tilde{f}(U, \epsilon),\ t > 0,\ x \in \Omega, \tag{G4}$$

where

$$\mathcal{L}U = \begin{pmatrix} d_1\Delta & 0 & 0 \\ 0 & d_1\Delta & 0 \\ 0 & 0 & d_2\Delta \end{pmatrix} U + L(0)U,$$

and

$$\begin{aligned} \tilde{f}(U, \epsilon) &= L(\epsilon)U - L(0)U + f(U, \epsilon) \\ &= \sum_{j_1+j_2+j_3+j_4+j_5 \geq 2} \frac{1}{j_1!j_2!j_3!j_4!j_5!} f_{j_1 j_2 j_3 j_4 j_5} \xi_1^{j_1} \xi_2^{j_2} \xi_3^{j_3} \epsilon_1^{j_4} \epsilon_2^{j_5} \end{aligned}$$

with

$$f(U, \epsilon) = \begin{pmatrix} f^{(1)}(U, \epsilon) \\ f^{(2)}(U, \epsilon) \\ f^{(3)}(U, \epsilon) \end{pmatrix},$$

in which

$$\begin{aligned} f^{(1)}(U, \epsilon) &= f_1(\xi_1 + I_{h2}, \xi_2 + R_{h2}, \xi_3 + I_{v2}) + \bar{\beta}_h I_{v2}\xi_2 - \bar{\beta}_h(N_h - I_{h2} - R_{h2})\xi_3 \\ &\quad + \left(\bar{\beta}_h I_{v2} + \frac{\delta}{(1 + (\alpha^* + \epsilon_1)I_{h2})^2} + r^* + \epsilon_2 + d_h\right)\xi_1, \\ f^{(2)}(U, \epsilon) &= 0, \\ f^{(3)}(U, \epsilon) &= f_3(\xi_1 + I_{h2}, \xi_2 + R_{h2}, \xi_3 + I_{v2}) - \bar{\beta}_v(N_v - I_{v2})\xi_1 - \theta\bar{\beta}_v(N_v - I_{v2})\xi_2 \\ &\quad + \left(\bar{\beta}_v(I_{h2} + \theta R_{h2}) + d_v\right)\xi_3. \end{aligned}$$

For $i \in \mathbb{N}_0$, denote

$$\mathcal{M}_i = \begin{pmatrix} -d_1 u_i - \bar{\beta}_h I_{v2} - d_h - r^* - \frac{\delta}{(1+\alpha^* I_{h2})^2} & -\bar{\beta}_h I_{v2} & \bar{\beta}_h m_5 \\ r^* & -d_1 u_i - (v + d_h) & 0 \\ \bar{\beta}_v(N_v - I_{v2}) & \theta\bar{\beta}_v(N_v - I_{v2}) & -d_2 u_i - m_3 \end{pmatrix}.$$

For any two vectors $\varphi, \psi \in \mathbb{R}^3$, define the product as $\langle \psi^{\mathrm{T}}, \varphi \rangle = \psi^{\mathrm{T}}\varphi$. Let

$$\Phi_0 = (\varphi_0, \overline{\varphi}_0),\ \Phi_{i^*} = \varphi_{i^*},\ \Psi_0 = col(\psi_0^{\mathrm{T}}, \overline{\psi}_0^{\mathrm{T}}),\ \Psi_{i^*} = \psi_{i^*}^{\mathrm{T}},$$

where $\varphi_0 = (\varphi_{01}, \varphi_{02}, \varphi_{03})^{\mathrm{T}} \in \mathbb{C}^3$, $\varphi_{i^*} = (\varphi_{i^*1}, \varphi_{i^*2}, \varphi_{i^*3})^{\mathrm{T}} \in \mathbb{R}^3$ are the eigenvectors relevant to the eigenvalues $i\omega_0$ and 0, respectively; $\psi_0 = (\psi_{01}, \psi_{02}, \psi_{03})^{\mathrm{T}} \in \mathbb{C}^3$, $\psi_{i^*} = (\psi_{i^*1}, \psi_{i^*2}, \psi_{i^*3})^{\mathrm{T}} \in \mathbb{R}^3$ are the corresponding adjoint eigenvectors. After some computations, acquire

$$\begin{aligned}
&\varphi_{01} = 1,\ \varphi_{02} = \frac{r^*}{i\omega_0 + d_h + v},\ \psi_{01} = \frac{1}{c_1},\ \psi_{03} = \frac{\bar{\beta}_h m_5}{c_1(m_3 - i\omega_0)},\\
&\varphi_{03} = \frac{r^*\bar{\beta}_h I_{v2}}{\bar{\beta}_h m_5(i\omega_0 + d_h + v)} + \frac{(\bar{\beta}_h I_{v2} + i\omega_0 + d_h + r^*)(1+\alpha^* I_{h2})^2 + \delta}{\bar{\beta}_h m_5(1+\alpha^* I_{h2})^2},\\
&\psi_{02} = \frac{1}{c_1 r^*}\left(\bar{\beta}_h I_{v2} + d_h + r^* + \frac{\delta}{(1+\alpha^* I_{h2})^2} - i\omega_0 - \frac{\bar{\beta}_v\bar{\beta}_h m_5(N_v - I_{v2})}{m_3 - i\omega_0}\right),\\
&\varphi_{i^*1} = 1,\ \varphi_{i^*2} = \frac{r^*}{d_1 u_{i^*} + d_h + v},\ \psi_{i^*1} = \frac{1}{c_2},\ \psi_{i^*3} = \frac{\bar{\beta}_h m_5}{c_2(d_2 u_{i^*} + m_3)},\\
&\varphi_{i^*3} = \frac{r^*\bar{\beta}_h I_{v2}}{\bar{\beta}_h m_5(d_1 u_{i^*} + d_h + v)} + \frac{(\bar{\beta}_h I_{v2} + d_1 u_{i^*} + d_h + r^*)(1+\alpha^* I_{h2})^2 + \delta}{\bar{\beta}_h m_5(1+\alpha^* I_{h2})^2},\\
&\psi_{i^*2} = \frac{1}{c_2 r^*}\left(d_1 u_{i^*} + \bar{\beta}_h I_{v2} + d_h + r^* + \frac{\delta}{(1+\alpha^* I_{h2})^2} - \frac{\bar{\beta}_v\bar{\beta}_h m_5(N_v - I_{v2})}{d_2 u_{i^*} + m_3}\right),
\end{aligned} \tag{G5}$$

where c_1, c_2 satisfy $\langle \Psi_0, \Phi_0 \rangle = I_2$ and $\langle \Psi_{i^*}, \Phi_{i^*} \rangle = 1$, respectively, in which I_2 is 2×2 identity matrix.

Carrying out Taylor expansion on $f(U, \varepsilon)$, the coefficients of second and third order terms are

$$\begin{aligned}
f_{20000} &= \begin{pmatrix} \frac{2\delta\alpha^*}{(1+\alpha^* I_{h2})^3} \\ 0 \\ 0 \end{pmatrix},\ f_{10100} = \begin{pmatrix} -\bar{\beta}_h \\ 0 \\ -\bar{\beta}_v \end{pmatrix},\\
f_{01100} &= \begin{pmatrix} -\bar{\beta}_h \\ 0 \\ -\theta\bar{\beta}_v \end{pmatrix},\ f_{30000} = \begin{pmatrix} \frac{-6\delta(\alpha^*)^2}{(1+\alpha^* I_{h2})^4} \\ 0 \\ 0 \end{pmatrix},
\end{aligned}$$

and all other coefficients equal $(0, 0, 0)^{\mathrm{T}}$. In light of the results in Song et al. (2016), acquire the following third-order truncated normal form

$$\begin{cases}
\dfrac{\mathrm{d}z_1}{\mathrm{d}t} = i\omega_0 z_1 + (B_{11}\epsilon_1 + B_{21}\epsilon_2)z_1 + B_{210}z_1^2 z_2 + B_{102}z_1 z_3^2,\\
\dfrac{\mathrm{d}z_2}{\mathrm{d}t} = -i\omega_0 z_2 + (\bar{B}_{11}\epsilon_1 + \bar{B}_{21}\epsilon_2)z_2 + \bar{B}_{210}z_1 z_2^2 + \bar{B}_{102}z_2 z_3^2,\\
\dfrac{\mathrm{d}z_3}{\mathrm{d}t} = (B_{13}\epsilon_1 + B_{23}\epsilon_2)z_3 + B_{111}z_1 z_2 z_3 + B_{003}z_3^3,
\end{cases} \tag{G6}$$

where

$$B_{210} = C_{210} + \frac{3}{2}(D_{210} + E_{210}),\ B_{102} = C_{102} + \frac{3}{2}(D_{102} + E_{102}),$$

$$B_{111} = C_{111} + \frac{3}{2}(D_{111} + E_{111}),\ B_{003} = C_{003} + \frac{3}{2}(D_{003} + E_{003}),$$

with

$$\begin{aligned}
C_{210} &= \frac{1}{6l\pi}\psi_0^{\mathrm{T}} A_{210},\ C_{102} = \frac{1}{6l\pi}\psi_0^{\mathrm{T}} A_{102},\ C_{111} = \frac{1}{6l\pi}\psi_{i^*}^{\mathrm{T}} A_{111},\ C_{003} = \frac{1}{4l\pi}\psi_{i^*}^{\mathrm{T}} A_{003},\\
D_{210} &= \frac{1}{6l\pi\omega_0 i}\left(-(\psi_0^{\mathrm{T}} A_{200})(\psi_0^{\mathrm{T}} A_{110}) + |\psi_0^{\mathrm{T}} A_{110}|^2 + \frac{2}{3}|\psi_0^{\mathrm{T}} A_{020}|^2\right),\\
D_{102} &= \frac{1}{6l\pi\omega_0 i}\left(-2(\psi_0^{\mathrm{T}} A_{200})(\psi_0^{\mathrm{T}} A_{002}) + (\psi_0^{\mathrm{T}} A_{110})(\overline{\psi}_0^{\mathrm{T}} A_{002}) + 2(\psi_0^{\mathrm{T}} A_{002})(\psi_{i^*}^{\mathrm{T}} A_{101})\right),\\
D_{111} &= -\frac{1}{3l\pi\omega_0} Im((\psi_{i^*}^{\mathrm{T}} A_{101})(\psi_0^{\mathrm{T}} A_{110})),\ D_{003} = -\frac{1}{3l\pi\omega_0} Im((\psi_{i^*}^{\mathrm{T}} A_{101})(\psi_0^{\mathrm{T}} A_{002})),\\
E_{210} &= \frac{1}{3\sqrt{l\pi}}\psi_0^{\mathrm{T}}\Big((f_{20000}\varphi_{01} + f_{11000}\varphi_{02} + f_{10100}\varphi_{03})h^{(1)}_{0110}\\
&\quad +(f_{11000}\varphi_{01} + f_{02000}\varphi_{02} + f_{01100}\varphi_{03})h^{(2)}_{0110}\\
&\quad +(f_{10100}\varphi_{01} + f_{01100}\varphi_{02} + f_{00200}\varphi_{03})h^{(3)}_{0110}\\
&\quad +(f_{20000}\overline{\varphi}_{01} + f_{11000}\overline{\varphi}_{02} + f_{10100}\overline{\varphi}_{03})h^{(1)}_{0200}\\
&\quad +(f_{11000}\overline{\varphi}_{01} + f_{02000}\overline{\varphi}_{02} + f_{01100}\overline{\varphi}_{03})h^{(2)}_{0200}\\
&\quad +(f_{10100}\overline{\varphi}_{01} + f_{01100}\overline{\varphi}_{02} + f_{00200}\overline{\varphi}_{03})h^{(3)}_{0200}\Big),\\
E_{102} &= \frac{1}{3\sqrt{l\pi}}\psi_0^{\mathrm{T}}\Big((f_{20000}\varphi_{01} + f_{11000}\varphi_{02} + f_{10100}\varphi_{03})h^{(1)}_{0002}\\
&\quad +(f_{11000}\varphi_{01} + f_{02000}\varphi_{02} + f_{01100}\varphi_{03})h^{(2)}_{0002}\\
&\quad +(f_{10100}\varphi_{01} + f_{01100}\varphi_{02} + f_{00200}\varphi_{03})h^{(3)}_{0002}\\
&\quad +(f_{20000}\varphi_{i^*1} + f_{11000}\varphi_{i^*2} + f_{10100}\varphi_{i^*3})h^{(1)}_{i^*101}\\
&\quad +(f_{11000}\varphi_{i^*1} + f_{02000}\varphi_{i^*2} + f_{01100}\varphi_{i^*3})h^{(2)}_{i^*101}\\
&\quad +(f_{10100}\varphi_{i^*1} + f_{01100}\varphi_{i^*2} + f_{00200}\varphi_{i^*3})h^{(3)}_{i^*101}\Big),\\
E_{111} &= \frac{1}{3\sqrt{l\pi}}\psi_{i^*}^{\mathrm{T}}\Big((f_{20000}\varphi_{01} + f_{11000}\varphi_{02} + f_{10100}\varphi_{03})h^{(1)}_{i^*011}\\
&\quad +(f_{11000}\varphi_{01} + f_{02000}\varphi_{02} + f_{01100}\varphi_{03})h^{(2)}_{i^*011}\\
&\quad +(f_{10100}\varphi_{01} + f_{01100}\varphi_{02} + f_{00200}\varphi_{03})h^{(3)}_{i^*011}\\
&\quad +(f_{20000}\overline{\varphi}_{01} + f_{11000}\overline{\varphi}_{02} + f_{10100}\overline{\varphi}_{03})h^{(1)}_{i^*101}\\
&\quad +(f_{11000}\overline{\varphi}_{01} + f_{02000}\overline{\varphi}_{02} + f_{01100}\overline{\varphi}_{03})h^{(2)}_{i^*101}\\
&\quad +(f_{10100}\overline{\varphi}_{01} + f_{01100}\overline{\varphi}_{02} + f_{00200}\overline{\varphi}_{03})h^{(3)}_{i^*101}\Big)\\
&\quad + \psi_{i^*}^{\mathrm{T}}(f_{20000}\varphi_{i^*1} + f_{11000}\varphi_{i^*2} + f_{10100}\varphi_{i^*3})\left(\frac{1}{3\sqrt{l\pi}}h^{(1)}_{0110} + \frac{1}{3\sqrt{2l\pi}}h^{(1)}_{(2i^*)110}\right)\\
&\quad + \psi_{i^*}^{\mathrm{T}}(f_{1100}\varphi_{i^*1} + f_{02000}\varphi_{i^*2} + f_{01100}\varphi_{i^*3})\left(\frac{1}{3\sqrt{l\pi}}h^{(2)}_{0110} + \frac{1}{3\sqrt{2l\pi}}h^{(2)}_{(2i^*)110}\right)\\
&\quad + \psi_{i^*}^{\mathrm{T}}(f_{10100}\varphi_{i^*1} + f_{01100}\varphi_{i^*2} + f_{00200}\varphi_{i^*3})\left(\frac{1}{3\sqrt{l\pi}}h^{(3)}_{0110} + \frac{1}{3\sqrt{2l\pi}}h^{(3)}_{(2i^*)110}\right),
\end{aligned}$$

$$
\begin{aligned}
E_{003} = {} & \psi_{i^*}^{\mathrm{T}}(f_{20000}\varphi_{i^*1} + f_{11000}\varphi_{i^*2} + f_{10100}\varphi_{i^*3})\left(\frac{1}{3\sqrt{l\pi}}h_{0002}^{(1)} + \frac{1}{3\sqrt{2l\pi}}h_{(2i^*)002}^{(1)}\right) \\
& + \psi_{i^*}^{\mathrm{T}}(f_{11000}\varphi_{i^*1} + f_{02000}\varphi_{i^*2} + f_{01100}\varphi_{i^*3})\left(\frac{1}{3\sqrt{l\pi}}h_{0002}^{(2)} + \frac{1}{3\sqrt{2l\pi}}h_{(2i^*)002}^{(2)}\right) \\
& + \psi_{i^*}^{\mathrm{T}}(f_{10100}\varphi_{i^*1} + f_{01100}\varphi_{i^*2} + f_{00200}\varphi_{i^*3})\left(\frac{1}{3\sqrt{l\pi}}h_{0002}^{(3)} + \frac{1}{3\sqrt{2l\pi}}h_{(2i^*)002}^{(3)}\right),
\end{aligned}
$$

with

$$
\begin{aligned}
h_{0200} &= \frac{1}{\sqrt{l\pi}}(2\omega_0 i\mathcal{I} - \mathcal{M}_0)^{-1}(A_{200} - \psi_0^{\mathrm{T}}A_{200}\varphi_0 - \overline{\psi}_0^{\mathrm{T}}A_{200}\overline{\varphi}_0), \\
h_{0020} &= \frac{1}{\sqrt{l\pi}}(-2\omega_0 i\mathcal{I} - \mathcal{M}_0)^{-1}(A_{020} - \psi_0^{\mathrm{T}}A_{020}\varphi_0 - \overline{\psi}_0^{\mathrm{T}}A_{020}\overline{\varphi}_0), \\
h_{0002} &= \frac{1}{\sqrt{l\pi}}(-\mathcal{M}_0)^{-1}(A_{002} - \psi_0^{\mathrm{T}}A_{002}\varphi_0 - \overline{\psi}_0^{\mathrm{T}}A_{002}\overline{\varphi}_0), \\
h_{0110} &= \frac{1}{\sqrt{l\pi}}(-\mathcal{M}_0)^{-1}(A_{110} - \psi_0^{\mathrm{T}}A_{110}\varphi_0 - \overline{\psi}_0^{\mathrm{T}}A_{110}\overline{\varphi}_0), \\
h_{i^*101} &= \frac{1}{\sqrt{l\pi}}(i\omega_0\mathcal{I} - \mathcal{M}_{i^*})^{-1}(A_{101} - \psi_{i^*}^{\mathrm{T}}A_{101}\varphi_{i^*}), \\
h_{i^*011} &= \frac{1}{\sqrt{l\pi}}(-i\omega_0\mathcal{I} - \mathcal{M}_{i^*})^{-1}(A_{011} - \psi_{i^*}^{\mathrm{T}}A_{011}\varphi_{i^*}), \\
h_{(2i^*)002} &= \frac{1}{\sqrt{2l\pi}}(-\mathcal{M}_{2i^*})^{-1}A_{002},\ h_{(2i^*)110} = (0,0,0)^{\mathrm{T}}.
\end{aligned}
$$

Moreover,

$$
\begin{aligned}
A_{200} = {} & f_{20000}\varphi_{01}^2 + 2f_{11000}\varphi_{01}\varphi_{02} + 2f_{10100}\varphi_{01}\varphi_{03} + f_{02000}\varphi_{02}^2 \\
& + 2f_{01100}\varphi_{02}\varphi_{03} + f_{00200}\varphi_{03}^2 = \overline{A}_{020}, \\
A_{002} = {} & f_{20000}\varphi_{i^*1}^2 + 2f_{11000}\varphi_{i^*1}\varphi_{i^*2} + 2f_{10100}\varphi_{i^*1}\varphi_{i^*3} + f_{02000}\varphi_{i^*2}^2 \\
& + 2f_{01100}\varphi_{i^*2}\varphi_{i^*3} + f_{00200}\varphi_{i^*3}^2, \\
A_{110} = {} & 2(f_{20000}|\varphi_{01}|^2 + 2f_{11000}Re(\varphi_{01}\overline{\varphi}_{02}) + 2f_{10100}Re(\varphi_{01}\overline{\varphi}_{03}) + f_{02000}|\varphi_{02}|^2 \\
& + 2f_{01100}Re(\varphi_{02}\overline{\varphi}_{03}) + f_{00200}|\varphi_{03}|^2), \\
A_{101} = {} & 2\,(f_{20000}\varphi_{i^*1}\varphi_{01} + f_{11000}(\varphi_{i^*2}\varphi_{01} + \varphi_{i^*1}\varphi_{02}) + f_{10100}(\varphi_{i^*3}\varphi_{01} + \varphi_{i^*1}\varphi_{03}) \\
& + f_{02000}\varphi_{i^*2}\varphi_{02} + f_{01100}(\varphi_{i^*3}\varphi_{02} + \varphi_{i^*2}\varphi_{03}) + f_{00200}\varphi_{i^*3}\varphi_{03}) = \overline{A}_{011},
\end{aligned}
$$

and

$$
\begin{aligned}
A_{210} = 3\Big(& f_{30000}|\varphi_{01}|^2\varphi_{01} + f_{03000}|\varphi_{02}|^2\varphi_{02} + f_{00300}|\varphi_{03}|^2\varphi_{03} \\
& + f_{21000}(2|\varphi_{01}|^2\varphi_{02} + \varphi_{01}^2\overline{\varphi}_{02}) + f_{20100}(2|\varphi_{01}|^2\varphi_{03} + \varphi_{01}^2\overline{\varphi}_{03}) \\
& + f_{12000}(2\varphi_{01}|\varphi_{02}|^2 + \overline{\varphi}_{01}\varphi_{02}^2) + f_{10200}(2\varphi_{01}|\varphi_{03}|^2 + \overline{\varphi}_{01}\varphi_{03}^2) \\
& + f_{02100}(2|\varphi_{02}|^2\varphi_{03} + \varphi_{02}^2\overline{\varphi}_{03}) + f_{01200}(2\varphi_{02}|\varphi_{03}|^2 + \overline{\varphi}_{02}\varphi_{03}^2)
\end{aligned}
$$

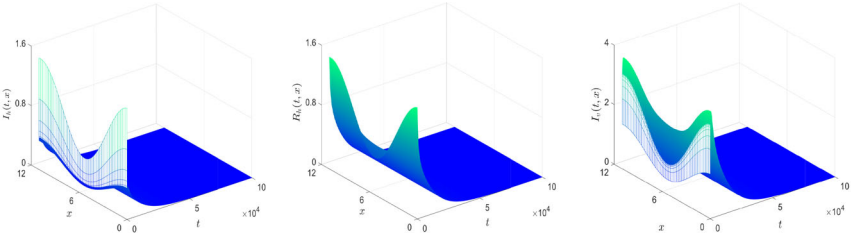

(a) The initial conditions are $I_h(0,x) = 1 + 0.5cos(0.6x)$, $R_h(0,x) = 1 + 0.5cos(0.6x)$ and $I_v(0,x) = 1 + 0.5cos(0.6x)$.

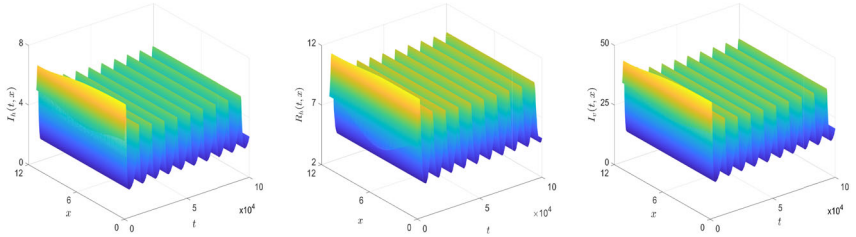

(b) The initial conditions are $I_h(0,x) = 6.2903 + cos(0.6x)$, $R_h(0,x) = 7.13 + cos(0.6x)$ and $I_v(0,x) = 29.88 + cos(0.6x)$.

Fig. 14 When $(\epsilon_1, \epsilon_2) = (8.0559 \times 10^{-4}, 5.2207 \times 10^{-5}) \in$ II, there are a stable E_0 and a stable spatially homogeneous periodic solution

$$
\begin{aligned}
&+2f_{11100}(\overline{\varphi}_{01}\varphi_{02}\varphi_{03} + \varphi_{01}\overline{\varphi}_{02}\varphi_{03} + \varphi_{01}\varphi_{02}\overline{\varphi}_{03}))\,,\\
A_{102} = 3\Big(&f_{30000}\varphi_{01}\varphi_{i*1}^2 + f_{03000}\varphi_{02}\varphi_{i*2}^2 + f_{00300}\varphi_{03}\varphi_{i*3}^2\\
&+f_{21000}(2\varphi_{01}\varphi_{i*1}\varphi_{02} + \varphi_{i*1}^2\varphi_{02}) + f_{20100}(2\varphi_{01}\varphi_{i*1}\varphi_{03} + \varphi_{i*1}^2\varphi_{03})\\
&+f_{12000}(2\varphi_{i*1}\varphi_{02}\varphi_{i*2} + \varphi_{01}\varphi_{i*2}^2) + f_{10200}(2\varphi_{i*1}\varphi_{03}\varphi_{i*3} + \varphi_{01}\varphi_{i*3}^2)\\
&+f_{02100}(2\varphi_{02}\varphi_{i*2}\varphi_{i*3} + \varphi_{i*2}^2\varphi_{03}) + f_{01200}(2\varphi_{i*2}\varphi_{03}\varphi_{i*3} + \varphi_{02}\varphi_{i*3}^2)\\
&+2f_{11100}(\varphi_{01}\varphi_{i*2}\varphi_{i*3} + \varphi_{i*1}\varphi_{02}\varphi_{i*3} + \varphi_{i*1}\varphi_{i*2}\varphi_{03}))\,,\\
A_{003} = &f_{30000}\varphi_{i*1}^3 + f_{03000}\varphi_{i*2}^3 + f_{00300}\varphi_{i*3}^3 + 3f_{21000}\varphi_{i*1}^2\varphi_{i*2} + 3f_{20100}\varphi_{i*1}^2\varphi_{i*3}\\
&+3f_{12000}\varphi_{i*1}\varphi_{i*2}^2 + 3f_{10200}\varphi_{i*1}\varphi_{i*3}^2 + 3f_{02100}\varphi_{i*2}^2\varphi_{i*3}\\
&+3f_{01200}\varphi_{i*2}\varphi_{i*3}^2 + 6f_{11100}\varphi_{i*1}\varphi_{i*2}\varphi_{i*3},\\
A_{111} = 6\Big(&f_{30000}|\varphi_{01}|^2\varphi_{i*1} + f_{03000}|\varphi_{02}|^2\varphi_{i*2} + f_{00300}|\varphi_{03}|^2\varphi_{i*3}\\
&+f_{21000}(2Re(\varphi_{01}\overline{\varphi}_{02})\varphi_{i*1} + |\varphi_{01}|^2\varphi_{i*2})\\
&+f_{20100}(2Re(\varphi_{01}\overline{\varphi}_{03})\varphi_{i*1} + |\varphi_{01}|^2\varphi_{i*3})\\
&+f_{12000}(2Re(\varphi_{01}\overline{\varphi}_{02})\varphi_{i*2} + |\varphi_{02}|^2\varphi_{i*1})\\
&+f_{10200}(2Re(\varphi_{01}\overline{\varphi}_{03})\varphi_{i*3} + |\varphi_{03}|^2\varphi_{i*1})\\
&+f_{02100}(2Re(\varphi_{02}\overline{\varphi}_{03})\varphi_{i*2} + |\varphi_{02}|^2\varphi_{i*3})\\
&+f_{01200}(2Re(\varphi_{02}\overline{\varphi}_{03})\varphi_{i*3} + |\varphi_{03}|^2\varphi_{i*2})
\end{aligned}
$$

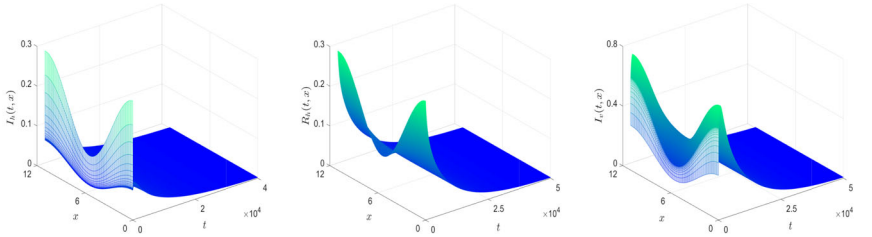

(a) The initial conditions are $I_h(0,x) = 0.2 + 0.1cos(0.6x)$, $R_h(0,x) = 0.2 + 0.1cos(0.6x)$ and $I_v(0,x) = 0.2 + 0.1cos(0.6x)$.

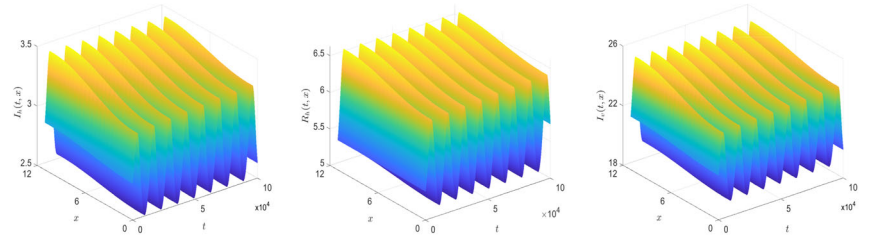

(b) The initial conditions are $I_h(0,x) = 2.8 - 0.01cos(0.3x)$, $R_h(0,x) = 5.4 - 0.01cos(0.3x)$ and $I_v(0,x) = 21 - 0.1cos(0.3x)$.

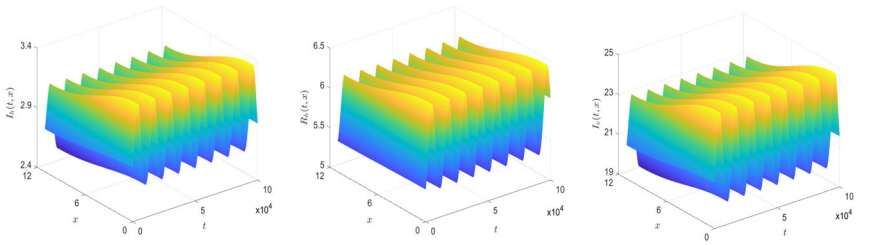

(c) The initial conditions are $I_h(0,x) = 2.8 - 0.01cos(0.3x)$, $R_h(0,x) = 5.4 - 0.01cos(0.3x)$ and $I_v(0,x) = 21 + 0.1cos(0.3x)$.

Fig. 15 When $(\epsilon_1, \epsilon_2) = (-7.7102 \times 10^{-4}, -7.27 \times 10^{-5}) \in$ IV, system (5) has a stable E_0 and a pair of stable spatially inhomogeneous periodic solutions

$$+2f_{11100}(Re(\varphi_{01}\overline{\varphi}_{02})\varphi_{i^*3} + Re(\varphi_{01}\overline{\varphi}_{03})\varphi_{i^*2} + Re(\varphi_{02}\overline{\varphi}_{03})\varphi_{i^*1})) .$$

In addition,

$$B_{11} = \psi_0^{\mathrm{T}} L_1^{(1,0)}(\varphi_0),\ B_{21} = \psi_0^{\mathrm{T}} L_1^{(0,1)}(\varphi_0),$$
$$B_{13} = \psi_{i^*}^{\mathrm{T}} L_1^{(1,0)}(\varphi_{i^*}),\ B_{23} = \psi_{i^*}^{\mathrm{T}} L_1^{(0,1)}(\varphi_{i^*}),$$

where

$$L_1^{(1,0)} = \begin{pmatrix} \frac{2\delta I_{h2}}{(1+\alpha^* I_{h2})^3} & 0 & 0 \\ 0 & 0 & 0 \\ 0 & 0 & 0 \end{pmatrix},\ L_1^{(0,1)} = \begin{pmatrix} -1 & 0 & 0 \\ 1 & 0 & 0 \\ 0 & 0 & 0 \end{pmatrix}.$$

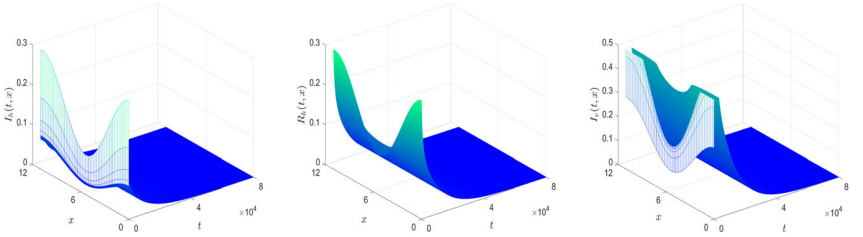

(a) The initial conditions are $I_h(0,x) = 0.2 + 0.1cos(0.6x)$, $R_h(0,x) = 0.2 + 0.1cos(0.6x)$ and $I_v(0,x) = 0.2 + 0.1cos(0.6x)$.

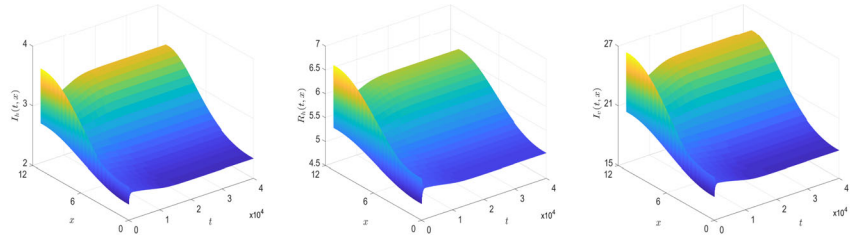

(b) The initial conditions are $I_h(0,x) = 2.9715 - 0.6855cos(0.3x)$, $R_h(0,x) = 5.7045 - 0.7405cos(0.3x)$ and $I_v(0,x) = 21.96 - 4.46cos(0.3x)$.

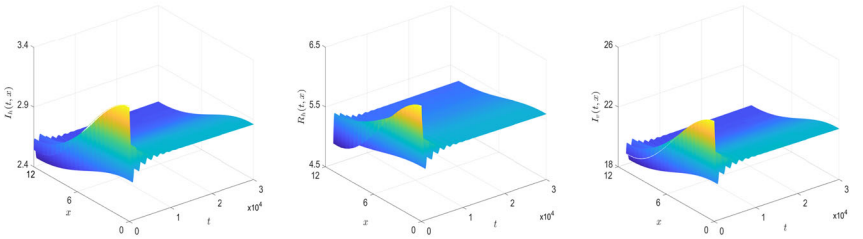

(c) The initial conditions are $I_h(0,x) = 2.9715 + 0.4cos(0.3x)$, $R_h(0,x) = 5.7045 + 0.7405cos(0.3x)$ and $I_v(0,x) = 21.96 + 2.8cos(0.3x)$.

Fig. 16 When $(\epsilon_1, \epsilon_2) = (-8.9791 \times 10^{-4}, -5.17 \times 10^{-5}) \in$ VI, E_0 and spatial inhomogeneous steady states are stable

Appendix H: Multi-stability of system (5) in regions II, IV and VI:

The part is devoted to presenting dynamics of system (5) in regions II, IV and VI. If $(\epsilon_1, \epsilon_2) \in$ II, then system (33) admits an unstable equilibrium J_0 and a stable equilibrium J_1. Correspondingly, when the parameter vector (ϵ_1, ϵ_2) passes through curve F_0 from I to II, the stability of E_2 for system (5) changes and a stable spatially homogeneous periodic solution appears. This indicates that system (5) presents periodic pattern for appropriate initial value. In the case, malaria is mainly manifested as disappearance or periodic outbreak (see Fig. 14).

When $(\epsilon_1, \epsilon_2) \in$ IV, system (33) admits four unstable equilibria J_0, J_1, $J_2^{\pm}$, and a pair of stable equilibria $J_3^{\pm}$. Accordingly, as the parameters ϵ_1, ϵ_2 pass through curve

K_1 from III to IV, a pair of stable spatially inhomogeneous periodic solutions emerge, and the spatially homogeneous periodic solution becomes unstable at the same time. Besides, the stability of E_0 and E_2 is same as that in II. This concludes that system (5) exhibits tristability and spatiotemporal patterns with appropriate initial conditions shown in Fig. 15.

When $(\epsilon_1, \epsilon_2) \in$ VI, system (33) admits a unstable equilibria J_0, and a pair of stable equilibria $J_2^{\pm}$. Then, as the parameter vector (ϵ_1, ϵ_2) passes through curve K_2 and moves to VI, the stable spatially inhomogeneous periodic solution disappears. There are a pair of stable spatial inhomogeneous steady states. Besides, the stability of E_0 and E_2 is same as that in II. In this case, system (5) also exhibits tristability (see Fig. 16).

References

Abboubakar H, Kamgang JC, Nkamba LN, Tieudjo D (2018) Bifurcation thresholds and optimal control in transmission dynamics of arboviral diseases. J Math Biol 76:379–427

An LTT, Jäger W (2014) A quantitative model of population dynamics in malaria with drug treatment. J Math Biol 69:659–685

Anita S, Capasso V (2012) Stabilization of a reaction-diffusion system modelling malaria transmission. Discrete Contin Dyn Syst Ser B 17(6):1673–1684

Bai ZG, Peng R, Zhao XQ (2018) A reaction-diffusion malaria model with seasonality and incubation period. J Math Biol 77:201–228

Becker N, Petrić D, Zgomba M, Boase C, Dahl C, Madon M, Kaiser A (2010) Mosquitoes and their control. Springer, Berlin

Bousema T, Okell L, Shekalaghe S, Griffin JT, Omar S, Sawa P, Sutherland C, Sauerwein R, Ghani AC, Drakeley C (2010) Revisiting the circulation time of Plasmodium falciparum gametocytes: molecular detection methods to estimate the duration of gametocyte carriage and the effect of gametocytocidal drugs. Malar J 9:136

Brauer F, Castillo-Chavez C (2012) Mathematical models in population biology and epidemiology. Springer, New York

Burundi Ministry of Public Health and the Fight Against AIDS (2023) Bulletins. http://minisante.bi/. Accessed 1 Jan 2023

Castillo-Chavez C, Song BJ (2004) Dynamical models of tuberculosis and their applications. Math Biosci Eng 1:361–404

Chitnis N, Hyman JM, Cushing JM (2008) Determining important parameters in the spread of malaria through the sensitivity analysis of a mathematical model. Bull Math Biol 70(5):1272–1296

Feng ZL, Yi YF, Zhu HP (2004) Fast and slow dynamics of malaria and the S-gene frequency. J Dyn Differ Equ 16(4):869–896

Fenichel N (1979) Geometric singular perturbation theory for ordinary differential equations. J Differ Equ 31:53–98

Gao YX, Zhang WP, Liu D, Xiao YJ (2017) Bifurcation analysis of an SIRS epidemic model with standard incidence rate and standard treatment function. J Appl Anal Comput 7(3):1070–1094

Guckenheimer J, Holmes P (1983) Nonlinear oscillations, dynamical systems, and bifurcations of vector fields. Springer, New York

Gutierrez JB, Galinski MR, Cantrell S, Voit EO (2015) From within host dynamics to the epidemiology of infectious disease scientific overview and challenges. Math Biosci 270:143–155

Hu ZY, Teng ZD, Jiang HJ (2012) Stability analysis in a class of discrete SIRS epidemic models. Nonlinear Anal Real World Appl 13(5):2017–2033

Laman M, Davis TME, Manning L (2014) Confirming cerebral malaria deaths in resource-limited settings. Am J Trop Med Hyg 90(2):192

Li S, Yuan SL, Jin Z, Wang H (2023) Bifurcation analysis in a diffusive predator-prey model with spatial memory of prey, Allee effect and maturation delay of predator. J Differ Equ 357:32–63

Lou YJ, Zhao XQ (2010) A climate-based malaria transmission model with structured vector population. SIAM J Appl Math 70(6):2023–2044
Lou YJ, Zhao XQ (2011) A reaction-diffusion malaria model with incubation period in the vector population. J Math Biol 62(4):543–568
Macdonald G (1952) The analysis of equilibrium in malaria. Trop Dis Bull 49(9):813–829
Macdonald G (1957) The epidemiology and control of malaria. Oxford University Press, London
Mtove G, Kimani J, Kisinza W, Makenga G, Mangesho P, Duparc S, Nakalembe M, Phiri KS, Orrico R, Rojo R, Vandenbroucke P (2018) Multiple-level stakeholder engagement in malaria clinical trials: addressing the challenges of conducting clinical research in resource-limited settings. Trials 19(1):190
Ross R (1911) The prevention of malaria. John Murray, London
Schlagenhauf P (2004) Malaria: from prehistory to present. Infect Dis Clin N Am 18(2):189–205
Shen H, Song YL, Wang H (2023) Bifurcations in a diffusive resource-consumer model with distributed memory. J Differ Equ 347:170–211
Shi L, Zhao HY, Wu DY (2021) Dynamical analysis for a reaction-diffusion HFMD model with nonsmooth saturation treatment function. Commun Nonlinear Sci 95:105593
Shi YY, Zhao HY (2021) Analysis of a two-strain malaria transmission model with spatial heterogeneity and vector-bias. J Math Biol 82(4):1–44
Shi YY, Zhao HY, Zhang XB (2022) Dynamics of a multi-strain malaria model with diffusion in a periodic environment. J Biol Dyn 16(1):766–815
Shi YY, Zhao HY, Zhang XB (2023) Threshold dynamics of an age-space structure vector-borne disease model with multiple transmission pathways. Commun Pure Appl Anal 22(5):1477–1516
Song YL, Zhang TH, Peng YH (2016) Turing–Hopf bifurcation in the reaction-diffusion equations and its applications. Commun Nonlinear Sci 33:229–258
Sun GQ (2012) Pattern formation of an epidemic model with diffusion. Nonlinear Dyn 69:1097–1104
Takoutsing E, Bowong S, Yemele D, Kurths J (2014) Effects of catastrophic anemia in an intra-host model of malaria. Int J Bifurc Chaos 24(7):1450105
Tatem AJ, Hay SI, Rogers DJ (2006) Global traffic and disease vector dispersal. Proc Natl Acad Sci USA 103(16):6242–6247
Wang H, Wang K, Kim YJ (2022) Spatial segregation in reaction-diffusion epidemic models. SIAM J Appl Math 82(5):1680–1709
Wang J, Zhao HY (2022) Bifurcation analysis of multiscale malaria model with Serratia AS1 bacteria and saturated treatment. Int J Bifurc Chaos 32(9):2250134
Wang K, Wang H, Zhao HY (2023) Aggregation and classification of spatial dynamics of vector-borne disease in advective heterogeneous environment. J Differ Equ 343:285–331
Wang K, Wang H, Zhao HY (2023) On the role of advection in a spatial epidemic model with general boundary conditions. J Differ Equ. https://doi.org/10.1016/j.jde.2023.12.016
Wang LP, Zhao HY, Oliva SM, Zhu HP (2017) Modeling the transmission and control of Zika in Brazil. Sci Rep-UK 7(1):7721
Wang WD, Zhao XQ (2012) Basic reproduction numbers for reaction-diffusion epidemic models. SIAM J Appl Dyn Syst 11(4):1652–1673
Wang WM, Gao XY, Cai YL, Shi HB, Fu SM (2018) Turing patterns in a diffusive epidemic model with saturated infection force. J Frankl Inst 355(15):7226–7245
Wang ZK, Wang H (2021) Bistable traveling waves in impulsive reaction–advection–diffusion models. J Differ Equ 285:17–39
World Health Organization (2023) Malaria. https://www.who.int/news-room/fact-sheets/detail/malaria. Accessed 1 July 2023
Xiang C, Huang JC, Wang H (2023) Bifurcations in Holling–Tanner model with generalist predator and prey refuge. J Differ Equ 343:495–529
Xin MZ, Wang BG (2021) Global dynamics of a reaction-diffusion malaria model. Nonlinear Anal Real World Appl 61:103332
Zha YJ, Jiang WH (2023) Global dynamics and asymptotic profiles for a degenerate Dengue fever model in heterogeneous environment. J Differ Equ 348:278–319
Zhang H, Wang H, Wei JJ (2023) Perceptive movement of susceptible individuals with memory. J Math Biol 86:65
Zhang X, Liu XN (2008) Backward bifurcation of an epidemic model with saturated treatment function. J Math Anal Appl 348(1):433–443

Zhao HY, Wang LP, Oliva SM, Zhu HP (2020) Modeling and dynamics analysis of Zika transmission with limited medical resources. Bull Math Biol 82:1–50
Zhao HY, Shi YY, Zhang XB (2022) Dynamic analysis of a malaria reaction–diffusion model with periodic delays and vector bias. Math Biosci Eng 19:2538–2574
Zhou LH, Fan M (2012) Dynamics of an SIR epidemic model with limited medical resources revisited. Nonlinear Anal Real World Appl 13(1):312–324
Zhou TT, Zhang WP, Lu QY (2014) Bifurcation analysis of an SIS epidemic model with saturated incidence rate and saturated treatment function. Appl Math Comput 226:288–305
Zhu LH, He L (2022) Two different approaches for parameter identification in a spatial-temporal rumor propagation model based on Turing patterns. Commun Nonlinear Sci 107:106174